# The effect of hyperbaric oxygen treatment on malignant progression in different breast cancer models *in vivo*

Kristine Yttersian Sletta

This thesis is submitted in partial fulfilment of the requirements for the degree of Master in Medical Biology – Human Physiology

Department of Biomedicine
University of Bergen

Spring 2016

# Acknowledgements

This master thesis was carried out at the Department of Biomedicine, University of Bergen during the period January 2015 to June 2016.

I would really like to express my gratitude towards my joyful and talented supervisor, Linda Stuhr. I cannot thank you enough for all your support, kindness and endurance through what has been a significant challenging time for me ($p>0.05$). Your engagement and academic guidance through this learning process has helped me tremendously.

Furthermore, I would like to extend my sincere appreciation to all of you in the matrix biology group. I would especially like to thank Trude Skogstrand, Tonje Sønstevold, Caroline Schmid and Gerd Salvesen who have supported and guided me through the laboratory work. Thank you Anne Nyhaug, for your excellent laboratory skills and contribution to this study.

Finally, I would like to thank my mum and dad for your ever-lasting patience, support and guidance throughout the years.

Last but not least, a big thank you to my partner in crime, Kristian Rørvik for your love and support.

TABLE OF CONTENTS

# LIST OF FIGURES

# LIST OF TABLES

# LIST OF FORMULAS

# Abbreviations

| | |
|---|---|
| Balb/c | Balb/cfC3H |
| BCSC | Breast cancer stem cells |
| C | Solubility of a gas at a given temperature in a liquid |
| CAM | Cell adhesion molecule |
| CV | Coefficient of variation |
| $CO_2$ | Carbon dioxide |
| DMBA | Dimethylbenz(a)anthracene |
| DMEM-D571 | Dulbecco´s Modified Eagles Medium |
| $ddH_2O$ | Double distilled water |
| ECM | Extracellular matrix |
| EDTA | Ethylenediaminetetraacetic acid |
| EMT | Epithelial to mesenchymal transition |
| FBS | Foetal bovine serum |
| HEPA | High efficiency particulate air |
| HER2 | Human epidermal growth factor receptor 2 |
| HIF1 | Hypoxia inducible factor 1 |
| HRP | Horse radish peroxidase |
| HBO | Hyperbaric oxygen |
| k | Henry´s law constant |
| LMS | Lung metastasis gene-expression signature |
| MDA-231 | MDA-MB-231 |
| MET | Mesenchymal to epithelial transition |

| | |
|---|---|
| MIC | Molecular Imaging Centre |
| mmHg | Millimeter mercury |
| MMP | Matrix metalloproteinase |
| $NaN_3$ | Sodium Azide |
| NC | Intensity value |
| Nod/scid | Non-obese diabetic/severe combined immunodeficient gamma |
| $NO_2$ | Nitrous oxide |
| $O_2$ | Oxygen |
| $P_{gas}$ | Partial pressure of that gas |
| PI | Propidium Iodide |
| PBS | Phosphate buffered saline |
| $pO_2$ | Arterial oxygen tension |
| RPM | Rounds per minute |
| ROI | Region of interest |
| SD | Standard deviation |
| SEM | Standard error mean |
| TBS | Tris buffered saline |
| TBS-T | Tris buffered saline-Tween® |
| TGF-β | Transforming growth factor beta |
| TNBC | Triple negative breast cancer |
| TPBC | Triple positive breast cancer |
| UHMS | Undersea and Hyperbaric Medical Society |

# Abstract

**Background**: Hypoxia is an important feature of most solid tumors and has shown to serve as a mediator for aggressive tumor growth and malignant progression of cancer. A correlation between low oxygen tension in tumors and increased predisposition for metastatic dissemination through epithelial to mesenchymal transition (EMT) has been reported. Research has shown significant anti-malignant effects of hyperbaric oxygen (HBO) treatment on chemically-induced and murine breast tumors. Thus, to establish whether HBO has a general effect on breast cancer, the overall aim of the present study was to target the hypoxic tumor microenvironment by enhancing oxygenation in human and murine breast cancer models. We investigated the effect of HBO on growth and metastasis of human and murine breast cancer cells *in vivo,* in addition to establish expression of major EMT markers and thus the metastatic potential.

**Methods**: A total of 24 balb/c and 12 nod/scid female mice were injected with 5 x $10^5$ breast cancer cells (human MDA-231 or murine 4T1 and 4T1-L) into the mammary fat pad at day 1. After tumor development the mice were divided into HBO treatment and control groups. Treatment consisted of 2.5 bar HBO exposure for 90 minutes, from day 7 post injection and every third day for 22, 25 or 53 days (4T1, 4T1-L and MDA-231 respectively) and non-treatment at normal atmospheric pressure. Mice with 4T1-L tumors were also used for biophotonic imaging to visualize cancer cells *in vivo.* Primary tumors were investigated for N- and E-cadherin expression by western blot and organs (lung and liver) were used for metastasis detection by histomorphometric quantification.

**Results and conclusion**: Repeated HBO treatment significantly reduced tumor growth and metastasis to lungs in the human (MDA-231) and murine (4T1-L) breast cancer model without affecting the murine 4T1 model. *In vivo* imaging of balb/c mice with 4T1-L tumors confirmed reduced tumor size compared to control but detected no metastases to distant sites. HBO treatment influenced EMT through downregulation of N-cadherin expression in human (MDA-231) primary tumors. The reduced metastatic potential could in part be attributed to this downregulation. Thus, HBO might be a possible potential adjuvant treatment of human breast cancer, although further research is needed.

# 1. Introduction

## 1.1 Cancer

Cancer is not one, but a group of diseases defined by abnormal cell growth (neoplasia), that acquire the ability to spread to other parts of the body. Over 100 types of cancer have been classified and the tissue of origin gives the cancer its distinguishing characteristics. Neoplastic cells generally grow to form solid masses of tissue called tumors, but some grow in cell suspension (e.g. leukemia's). Neoplastic cells can either be benign or malignant, and only the latter is synonymous with cancer (1). For the remaining part of the thesis malignant neoplasms are referred to as tumors. Tumor grading is a normal procedure during staging a cancer, and depends on how abnormal the tumor tissue morphology appears histologically. Tumors have a considerably increased rate of growth (proliferation) and show varying degrees of cell differentiation. Tumor cells that are poorly differentiated are called anaplastic cells. Normally, the grading system ranges from grade 1, where less than 25% of cells are anaplastic to grade 5, where over 75% of cells are anaplastic (1, 2). Despite the specific tumor heterogeneity, tumors share some common traits that will be described below.

### 1.1.1 Hallmarks of cancer

In 2000, Hanahan and Weinberg (3) described the "Hallmarks of cancer" to which they proposed six biological capabilities that define the development and progression of tumors. Since then, two emerging hallmarks and two enabling characteristics have been added to the list (4). Although the underlying cellular and molecular course of cancer is different, the end result is the same.

*1. Sustaining proliferative signaling*

Cancer cells acquire mutations that short circuit growth factor pathways, rendering them independent on external growth factor signaling. Normal growth regulation is therefore avoided, leading to unregulated proliferation.

*2. Evasion of growth inhibitory signals*

Maintaining homeostasis is avoided by interference with inhibitory pathways and mutated cancer cells do not respond to growth inhibitory signals. For example, the normal tumor suppressor gene p53 responds to intracellular stress and arrest the cell division cycle. However, a mutated p53 does not produce functional growth inhibitory proteins, and cell division is not under control.

*3. Evasion of apoptosis*

Normal cells undergo apoptosis to limit growth of DNA damaged cells. However, cancer cells can acquire apoptotic resistance through different mutations, and secrete anti-apoptotic signaling proteins.

*4. Unlimited replicative potential*

The activation of the enzyme telomerase by cancer cells maintains the length of telomeres, which allows the cell to replicate indefinitely.

*5. Angiogenesis*

Growing tumors are dependent on elevated blood supply to provide enough oxygen and nutrients to the increasing number of cells. They are therefore able to stimulate the formation of new blood vessels, called angiogenesis through activation of the “angiogenic switch” (5). An alteration between angiogenic inducers and inhibitors activate this switch and promote tumor growth.

*6. Invasion and metastasis*

Unlike normal cells, cancer cells do not maintain their location, but migrate and invade other tissues in the body by a process called metastasis. This process is responsible for most cancer-related deaths.

*7. Avoiding immune destruction*

An emerging hallmark is the strategy for cancer cells to evade attack and destruction by immune cells. Poorly immunogenic cells are able to replicate and escape "immunosurveillance". Furthermore, cancer cells have shown to reduce the immune response by secreting immunosuppressive factors such as transforming growth factor-beta (TGF-β) (6).

*8. Deregulating cellular energetics*

The second emerging hallmark represents a major reprogramming of cellular energy metabolism in order to support continuous growth and proliferation. In addition to switching to glycolysis for energy production, cancer cells can up-regulate specific transporters like GLUT1 thereby enhancing glucose utilization (7).

### 1.1.2 Enabling characteristics

*1. Tumor-promoting inflammation*

Recently, researchers have discovered that the tumor-associated inflammatory response is in fact enhancing tumorigenesis and progression. Studies have shown that T and B lymphocytes have functional tumor-promoting effects through regulation of the innate immune system (8), and that inflammatory cells contribute to enhancing capabilities (9, 10).

*2. Genomic instability*

The ability of tumor cells to acquire the hallmarks of cancer largely depends on multiple genetic alterations over time. Certain mutated genotypes confer an advantage to sub clones in order to facilitate sustained growth in the local tissue. The rate of mutation in tumor cells has been shown to increase during the course of tumorigenesis through heightened sensitivity to mutagenic agents. (11).

## 1.2 Breast Cancer

Breast cancer remains the most frequent type of cancer among females worldwide, with 1.67 million new patients diagnosed in 2012. It is the most leading cause of cancer mortality in females with more than 500 000 deaths annually (12). According to the Norwegian Cancer Registry, 31 651 new cancer cases were registered in the country in 2014. Over 3300 of these cases were breast cancers, making it the second most prevalent type after prostate cancer (13). It is far more dominant in western countries than in Africa, South America or Asia (12), and several causative agents have been implicated with the pathogenesis of breast cancer. These include age, genetics, family history, diet, smoking, alcohol, obesity, physical inactivity and endocrine factors (14). However, as with most types of cancer, the exact mechanisms behind cancer development are still unknown. Males can also develop breast tumors, however it is 100 times less common than among females. The risk of developing breast tumors in males is estimated to be 1 in 1,000, compared to an estimated 1 in 8 for women (12).

### 1.2.1 Anatomic characterization

The female breast consists of glandular tissue, milk-producing lobules and small ducts that carry milk to a reservoir that lies just beneath the nipple. Connective tissue and fatty

tissue surround the glands and ducts. Lymph vessels are also connected to the breast (Fig. 1) (15).

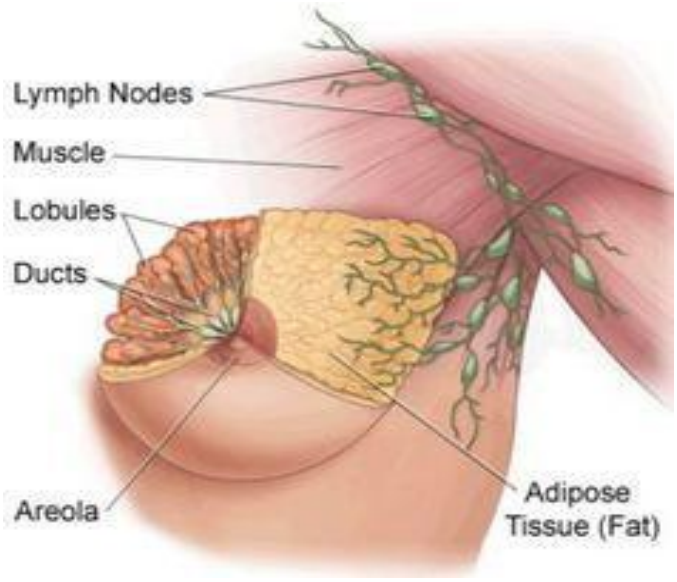


**Figure 1**: Anatomy of the female breast, frontal view. With permission (16).

Breast cancer usually arises in the cells lining the milk ducts (80%), but also in cells lining the lobules (10%). They start out as either ductal or lobular carcinomas in situ with increased risk of developing invasive breast carcinoma. In fewer cases (10%), breast cancer leads to inflammation by from blocked lymph vessels (inflammatory breast cancer) or cancer arises from connective tissues between the ducts and lobules (17).

### 1.2.3 Genetic characterization

Breast tumors contain oncogenes and/or tumor-suppressor genes that could induce cancer and promote aggressive tumor growth. These may be inherited or arise from spontaneous mutation. Note that tumor suppressor genes are recessive and require

knock-out of both alleles to lose its function, whilst oncogenes are dominant and require only one mutated allele to produce mutated protein product (1).

Specific inherited mutated genes have been identified as high penetrance susceptibility genes that confer an increased risk of developing breast cancer. About five to ten percent of breast cancer incidents develop from germ-line mutations in the BRCA1 and BRCA2 genes, located on chromosome 17 and chromosome 13, respectively. The risk for developing breast cancer for gene-positive patients is 57% for BRCA1 and 49% for BRCA2 (18). Normal functional versions of these genes produce tumor suppressor proteins that helps repair DNA damage. Mutated versions either produce dysfunctional proteins or do not express the protein at all (14). Consequently, to avoid developing breast cancer, many women with confirmed BRCA1 and BRCA2 mutations choose to undergo radical mastectomy and oophorectomy.

### 1.2.4 Subtypes

Research continues to demonstrate molecular and genetic differences in breast cancer, implying a demand to elucidate the unique characteristics of the primary tumor to better understand tumor-host interaction. Hence, breast cancer has been classified into subtypes that rely heavily upon the underlying molecular histopathological features of the primary tumor. More detailed molecular profiles of subtyping tumors have been proposed by researchers, however the most common types are outlined below. These subtypes differ vastly in behavior and respond differently to treatments.

*HER2 positive breast cancer*

Approximately 20-30% of breast tumors contain over-expression of the human epidermal growth factor receptor 2 (HER2) that results from the up-regulated HER2 oncogene. The action of the over-expressed HER2 results in uncontrolled cell growth and tumors tend to exhibit a more aggressive phenotype with higher recurrence rate

than HER2 negative breast cancers (1, 19). In addition, HER2 positive cancers seem to predict poorer prognosis and overall survival for patients. However, treatment with trastuzumab, a humanized monoclonal antibody targeting HER2 has shown to improve the prognosis of these aggressive cancers. Today, adjuvant trastuzumab therapy is therefore offered to cancer patients with “HER2” positive breast cancer in combination with chemotherapy (20, 21).

*Endocrine receptor-positive breast cancer*

Most breast cancers (80%) are “ER-positive”, meaning that the cancer cells grow in response to the hormone estrogen. Of these cases, approximately 65% also grow in response to progesterone, called “PR-positive”. ER-positive breast cancers respond well to hormone therapy that include estrogen receptor inhibitors (e.g. tamoxifen) and aromatase inhibitors for post-menopausal women (e.g letrozole) to lower estrogen levels (22). In addition, hormone ER-positive breast cancer is generally seen as treatable and manageable, especially if caught at an early stage.

*Triple positive breast cancer*

Breast cancers that are ER-positive, PR-positive and HER2 positive are referred to as triple positive breast cancers (TPBC). These cancer cells grow in response to the hormone estrogen, progesterone and contain the HER2 proto-oncogene, and thus, respond well to hormone therapy and HER2 inhibitors (23).

*Triple negative breast cancer*

Breast cancers which are endocrine receptor- and HER2-negative are referred to as triple negative breast cancer (TNBC). The TNBC cells do not express estrogen or progesterone receptors and do not contain HER2 over-expression. Consequently, due to the lack of effective targeted therapies previously mentioned, TNBC is difficult to treat (24). In addition, TNBC is associated with increased metastatic potential, high recurrence rate and decreased five-year survival rate. The standard treatment involves chemotherapy and radiotherapy, along with surgery. TNBC accounts for around 10-15%

of all breast cancers, in which younger women seem to have a higher risk of developing than older women (23, 25).

## 1.3 Metastasis

Metastasis is the spread of tumor cells from its primary site throughout the body and is a distinct characterization of malignant tumors. The process of metastasis is initiated when tumor cells lose their adhesive properties and detach from the primary tumor. They intravasate and migrate through the blood or lymphatic system. The circulating cancer cells finally adhere, proliferate and form micro-metastases at a distant site (1). This represents a major clinical problem in cancer treatment. In breast cancer, the primary tumor can often easily be removed surgically, however over 50% of tumors have metastasized at the time of diagnosis and often includes hundreds of metastases that are practically impossible to remove. Even 30% of cases initially diagnosed at an early stage will develop metastatic tumors months or years later (26). Metastatic spread of breast cancer is responsible for 90% of breast cancer-related deaths and thus represents the most important negative prognostic predictor. Perhaps the most lethal consequence of metastasis is the ability of tumor cells to compete with normal cells for nutrients and oxygen, which eventually impair normal organ function (1, 14).

Breast cancer metastasis usually occurs in lymph nodes, bone, lungs, liver and brain (27, 28). In theory, blood flow to organs in close proximity to the primary tumor is the most likely sites of metastasis. However, studies have shown that it metastasizes to bone more likely than blood flow/anatomy would suggest (1). In addition, breast cancer subtypes display a marked difference in metastatic patterns. TNBC show increased visceral metastases, meaning metastases to internal organs such as liver, lungs and body cavities. Hormone receptor-positive tumors however, tend to show increased metastases to bone. HER2-positive tumors show an increased tendency to metastasize to the brain more frequent than HER2-negative tumors (29). Although the exact

mechanisms behind these observations remain to be elucidated, a possible explanation is the so-called “seed and soil” theory. It suggests that tumor cells are “seeds” that need to be in a favoring microenvironment, being the “soil”. Furthermore, unique biochemical and physical characteristics of bone such as growth factors and acidic pH are properties that promotes tumor growth and could explain the increased observation of breast tumor cells in bone (30). Finally, an extensive review by Redig *et al. (27)* elucidating the complex molecular metastasis pattern of different breast cancer subtypes, suggested that future breast cancer treatment should focus more on targeting the specific processes that lead to metastasis.

Since metastasis is so detrimental and the metastatic pattern differ vastly according to breast cancer subtypes, recognition and understanding of the metastatic process and its contributors is paramount for developing new cancer treatments.

### 1.3.1 Epithelial to mesenchymal transition

Epithelial-to-Mesenchymal transition (EMT) is a fundamental biological process essential for embryogenesis. However, in tumor progression, EMT is thought to be an initiative and vital process in the metastatic cascade. EMT occurs when epithelial cells undergo series of biochemical changes to lose their adhesive properties and cell polarity. In preference, they acquire a mesenchymal phenotype, which include increased migratory capacity, invasiveness and an increased production of extracellular matrix (ECM) components (31, 32).

*Cell adhesion*

In order for the epithelial cells to lose their adhesive properties, mediating proteins like cell adhesion molecules (CAMs) and cadherins are thought to be involved. Cadherins are calcium dependent transmembrane proteins that normally form adherence junctions and together with CAMs, “hook” cells into place with each other extracellularly (1, 31). Several studies show that these molecules are key factors during metastasis. More

specifically, gain of N-cadherin and loss of E-cadherin is considered to contribute to enhanced invasiveness (33, 34). Interestingly, a transfection of the E-cadherin gene into metastatic epithelial cells rendered them non-invasive (35). The exact mechanism behind this step in EMT is poorly understood, but one plausible hypothesis is that gain of N-cadherin and loss of E-cadherin decreases cell-cell adhesiveness (Fig. 2).

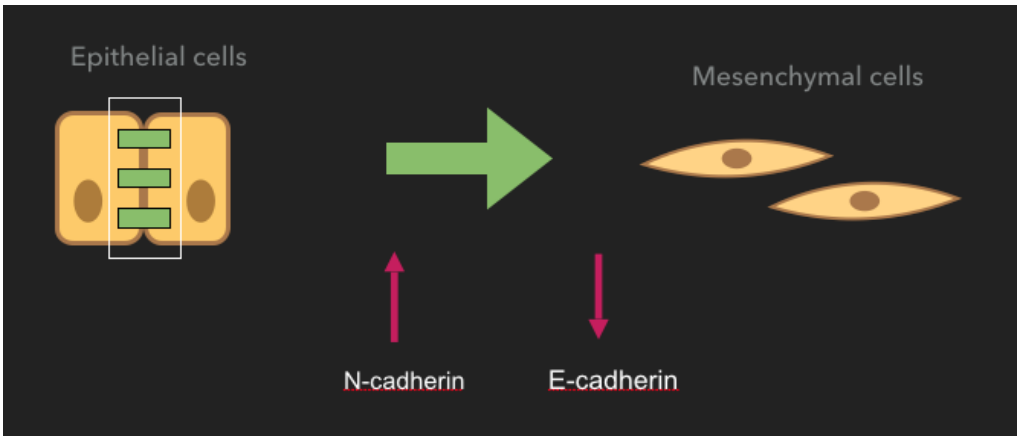


**Figure 2**: The epithelial to mesenchymal transition involving loss of adhesive properties through a gain in N-cadherin and loss of E-cadherin.

*Intravasation and transport*

Further, cancerous epithelial cells must break free from the ECM components that restrain them. Special integrins of the cell adhesion family are thought to be involved in the loss of cell-ECM interaction, and matrix metalloproteases (MMP´s) in the degradation of ECM components (32). The tumor cells are able to exit through the basement membrane (absent in the lymphatic system) and enter the blood or lymphatic system via penetration between the endothelial cells. In the circulation, the transport is one-way in the direction of flow and in the blood stream they are accompanied by platelets (1, 31).

*Extravasation and metastatic colonization*

The step for extravasation is the same as intravasation just in reverse. After successfully exiting though the endothelium and basement membrane, tumor cells can migrate into the surrounding stroma and form a secondary tumor at the secondary site (31). It has become evident that primary tumor cells orchestrate the development of a supportive microenvironment in secondary organs known as the “pre-metastatic niche” before the arrival of tumor cells. Tumor cells change the stromal host compartment through secretion of cytokines and growth factors which recruit and mobilize bone marrow derived cells to the pre-metastatic niche (36). When tumor cells arrive, the favorable microenvironment contributes to progressive growth and initiates angiogenesis that is essential for providing nutrients and oxygen (Fig. 3).

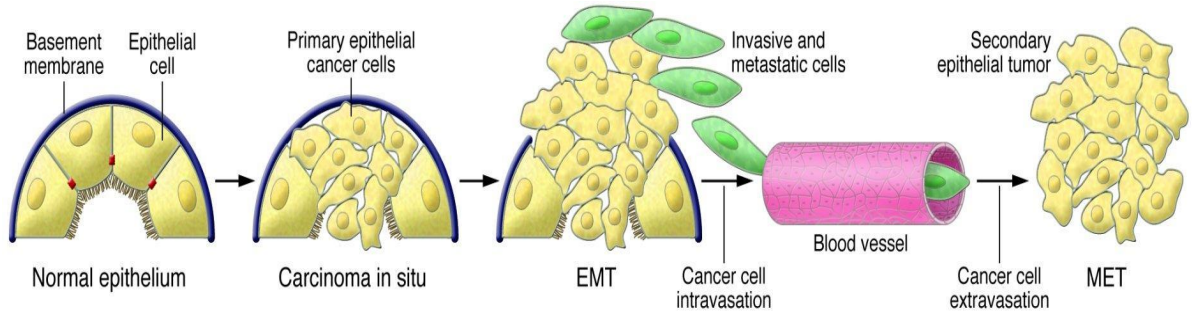


**Figure 3:** The contribution of EMT on cancer progression and metastasis. With permission (31).

Thus, the stromal microenvironment plays a major role in EMT which might demonstrate a more intricate tumor growth and progression that may challenge the current methods of treating metastatic cancer. Recent research has shown that hypoxic tumor cells condition pre-metastatic niches by secretion of factors that recruits certain myeloid cells and suppress natural killer cells (37). Hence, tumor cells and the stromal components are closely interacted, and the communication between them is bidirectional.

## 1.4 Tumor hypoxia

A common trait for most solid tumors is hypoxia, a condition where tissues are deprived of adequate oxygenation supply. Cells cannot normally survive without having a proximal vessel system that provides nutrients and oxygen, while removing waste products as well. The tumor vasculature is often disorganized and dysfunctional (irregular and sluggish blood flow) because the progressive tumor growth overrides the ability of the vasculature to adapt to the increasing oxygen demand (38). It also increases diffusion distances and induces tumor-associated anemia (39). Thus, without a functional vascular network, tumors are subjected to hypoxia. Solid tumors are, in fact, distinctively less oxygenated than the normal tissue from which they arose. Different areas of the tumor are subjected to different levels of hypoxia that would normally be toxic to cells, including tumor cells (40).

Hypothetically, hypoxia may limit cell growth and contribute to decreased tumor progression. Nevertheless, tumor cells display an impressive ability to adapt and undergo genetic changes that facilitate continuous survival and proliferation in the hypoxic microenvironment (41, 42). Thus, hypoxia serve as a mediator for aggressive tumor growth and has been associated with malignant progression (42, 43). In particular, hypoxia has emerged as a primary inducer of the angiogenic switch, which previously mentioned is a hallmark of cancer development (44). It stimulates an up-regulation of pro-angiogenic factors such as hypoxia inducible factor 1 (HIF1). HIF1 activates vascular endothelial growth factors (VEGF), inducing blood vessel formation in tumors (40, 45). In addition, hypoxic stimulation of HIF1 activates a number of target genes involved in various other cell processes crucial for tumor biology (46). In relation to breast cancer, HIF1 has shown to be over-expressed and associated with aggressive tumor growth (47). Several signaling pathways involved in cell proliferation have also shown to be under the influence of hypoxia and HIF1 (48). Hypoxic conditions also prompt tumor cells to switch from aerobic to anaerobic metabolism. Cells deprived of adequate oxygen supply employ glycolysis as their primary mechanism of energy production (49). Although p53-mediated apoptosis seems to be upregulated under

hypoxic conditions (50), tumor cells have acquired mechanisms to evade mediated cell death through induction of anti-apoptotic genes such as IAPS (51).

In addition, associations between hypoxic tumors and increased metastatic ability have been established (52, 53). Further, tumor hypoxia seem to predispose for increased tumor metastases through induction of EMT, where E- and N-cadherin plays a critical role (54, 55). Because the primary tumor cells and metastatic cells are similar morphologically, researchers have suggested that tumor cells regain epithelial properties at the secondary site, known as Mesenchymal-to-Epithelial transition (MET) (56). This transition has been linked to reduced tumor malignancy and invasiveness (57) .

Another important feature of hypoxic tumors; reduced arterial oxygen tension ($pO_2$), restricts organ and tissue function and can serve as an adverse prognostic factor. A study conducted by Hockel *et al. (58)* showed that hypoxic tumors (median $pO_2$<10mmHg) in patients with cervical cancer had an increased risk of malignancy and worse overall survival. Moreover, a more recent study showed hypoxia to be a marker for metastatic disease in patients and that hypoxic tumors (median $pO_2$<5mmHg) couldpredict progression-free survival of these patients (59).

Initially, tumor hypoxia was studied due to its contribution to radiation and cancer chemotherapy resistance (60, 61). However, as ongoing research demonstrated its negative prognostic factor involving tumor cell adaptation, growth and metastasis, it´s now considered one of the best target options in cancer treatments.

## 1.5 Hyperbaric Oxygen Treatment

Hyperbaric oxygen (HBO) treatment is a method of enhancing tissue oxygenation by administering 100% pure oxygen at increased atmospheric pressure, using a hyperbaric chamber and treating for one or more consecutive sessions. Generally, the atmospheric pressure is elevated to 2- 2,5 bar corresponding to 10-15 meters below sea level (62).

HBO enhances tissue oxygenation by exploiting the physical properties of gases under pressure. Since hemoglobin saturation is around 97% at normal ambient pressure, HBO will not impact the total hemoglobin oxygen concentration. Instead, increased partial oxygen pressure ($pO_2$) will push more oxygen into solution and expose tissues to elevated oxygen concentrations. This can be explained by Henry´s law:

Henry´s law (Fomula 1) states that the amount of a given gas dissolved in liquid is directly proportional to its partial pressure in equilibrium with the liquid at a given temperature.

**Fomula 1**: Henry´s law

$$C = k \times P_{gas}$$

- C = The solubility of a gas at a given temperature in a particular liquid,
- k = Henry´s law constant,
- $P_{gas}$ = the partial pressure of the gas

According to Henry´s law, exerting elevated ambient pressure magnifies the amount of dissolved oxygen in blood plasma (63). Administering 100% pure oxygen at normal ambient pressure (1 bar) enhances the amount of dissolved oxygen in plasma from 3.2 to 20.9 ml/1000ml blood. At 3 bar pure oxygen, the amount of dissolved oxygen in plasma will be 20 times higher than ambient pressure as shown in Table 1.

**Table 1:** Arterial oxygen pressures ($pO_2$) and dissolved oxygen concentrations in blood plasma at different pressures (normobaric and hyperbaric). Modified from Sahni *et al. (64)* .

| Pressure | % Oxygen | $pO_2$ (mmHg) | ml dissolved $O_2$ /1000 ml blood |
|---|---|---|---|
| 1 bar | 21% (normal air) | 159 | 3.2 |
| 1 bar | 100% | 760 | 20.9 |
| 2 bar | 100% | 1520 | 44.4 |
| 2.5 bar | 100% | 1900 | 56.2 |
| 3 bar | 100% | 2280 | 68 |

Resting tissue will excerpt 50-60 ml of oxygen per 1000 ml of blood assuming normal perfusion. Thus, increasing the pressure to 3 bar pure oxygen will hyper-saturate the blood with oxygen more than enough to meet resting tissue requirements without the contribution of hemoglobin (65). The dissolved oxygen even passes through obstructed areas where passage of red blood cells is limited. Additionally, the diffusion distance of oxygen through normal tissue is also considerably increased due to the increase in $pO_2$ (63). The amount of dissolved oxygen remains high for approximately 2-4 hours after administration of HBO treatment (66). Hence, HBO administration greatly enhances prolonged tissue oxygenation by elevated transport of soluble oxygen.

HBO treatment is well established and considered a safe treatment for humans, without side-effects up to 2.8 bar (67). It is the primary line of treatment for decompression sickness, and The Undersea and Hyperbaric Medical Society (UHMS) has approved HBOT for treating a total of 14 diseases and conditions (Table 2).

**Table 2**: Undersea and Hyperbaric Medical Society (UHMS) approved indications for hyperbaric oxygen treatment (68) .

| |
|---|
| Air or gas embolism |
| Carbon monoxide poisoning |
| Clostridial myositis myonecrosis |
| Crush injury, compartment syndrome and other acute ischemias |
| Decompression sickness |
| Arterial insufficiencies |
| Severe anemia |
| Intracranial abscess |
| Necrotizing soft tissue infections |
| Osteomyelitis |
| Delayed radiation injury |
| Compromised grafts and flaps |
| Acute thermal burn injury |
| Idiopathic sudden sensorineural hearing loss |

The beneficial mechanical effect of HBO treatment on decompression sickness and air embolism is reduction in bubble size by the increased pressure. For carbon monoxide poisoning, reversing hypoxia and competing with carbon monoxide for hemoglobin binding will treat the condition. In treatment of infections, HBO kills bacteria through recruitment of leukocytes and production of oxygen free radicals and facilitation of oxygen-dependent systems that induces certain antibiotics. HBO enhances wound healing by augmenting oxygen gradients next to ischemic wounds and induction of angiogenesis through oxygen-dependent ECM and collagen formation (62, 65). Even though HBO leads to vasoconstriction, blood flow significantly improves in ischemic tissue due to the increased oxygen carriage capacity in plasma. Thus, post-traumatic tissue edema is reduced, contributing to the treatment of crush injuries, compartment syndromes and burns (69).

In summary, HBO treatment has therapeutic effects on many pathological conditions through enhanced oxygen transport, induction of angiogenesis and stimulation of the

immune system. Perhaps the most positive effect comes from a reduction in hypoxia, enabling normal host responses to fight infection and disease.

## 1.6 HBO treatment and cancer

Our group has postulated a hypothesis saying that since tumor hypoxia represents increased malignancy through tumor progression and metastasis, reducing the hypoxic state of tumors could have opposing effects.

However, because increased tissue oxygenation enhances ECM matrix formation, and induction of angiogenesis, it was feared that it would actually promote tumor growth. Interestingly, comprehensive studies on the effect of HBO treatment on normal tissue imply that tumors differ in response from normal tissue. In 2003, a review by Feldmeier *et al. (70)* and Daruwalla *et al. (71)* some years later, concluded that there is no evidence for HBO tratment enhancing tumor malignancy. In 2012, Moen *et al. (72)* supplemented the previous reviews. No existing research has indicated enhanced tumor growth nor enhanced recurrence after HBO treatment. Alternately, they presented evidence that HBO treatment has an antiproliferative effect on certain tumor types, and suggested that it could be effective in breast cancer treatment. It has become well documented that HBO treatment reduces tumor growth compared to controls in breast tumor models (73). In addition, Moen *et al. (57)* reported that HBOT induced MET and lead to less aggressive tumor behavior in an in-vivo 7,12-Dimethylbenzanthracene (DMBA) - induced breast cancer model. Furthermore, they also showed a metabolic shift away from glycolysis to oxidative phosphorylation after HBO treatment. Hence, on that background HBO treatment might inhibit or reduce tumor metastases in breast cancer. In essence, since metastatic spread of tumors is responsible for most breast cancer-related deaths, it is of interest to evaluate whether HBO treatment could potentially significantly increase or prolong survival.

# 2. Aims

The overall aim of the present study was to target the hypoxic tumor microenvironment.

The following specific sub-aims were to:

1. Investigate the effect of hyperbaric oxygen therapy on the malignant progression of human (MDA-MB-231) and murine (4T1 and 4T1L) breast cancer cells in vivo.

2. Visualize potential metastases *in vivo* through biophotonic imaging

3. Elucidate if hyperbaric oxygen treatment would influence major epithelial to mesenchymal transition markers and thus the metastatic potential.

# 3. Methods and materials

## 3.1 Cell lines

A murine breast carcinoma cell line 4T1 and a human breast carcinoma cell line; MDA-MB-231 (MDA-231) obtained from the American Type Culture Collection (Rockville, MD, USA) was used. A 4T1 cell line engineered to express the firefly enzyme Luciferase (4T1-L) to allow tracking and quantification through bioluminescence was also used. This cell line was a gift from Professor James Lorentz, University of Bergen, Norway.

The murine 4T1 cell line was originally isolated from a spontaneous arising mammary tumor in a female Balb/cfC3H (Balb/c) mouse (74), while the MDA-231 cell line was originally isolated by pleural effusion from a 51 year-old Caucasian female with metastatic breast cancer (75).

Both cell lines are well characterized and known to metastasize to sites as in human breast cancer (lungs, lymph nodes, liver, bone and brain) via the haematogenous route in mice, making it a representable model for studying human breast cancer behavior (74, 76).

The 4T1 and 4T1-L cells were cultured with RPMI-1640 medium, and the MDA-231 cells were cultured with Dulbecco´s Modified Eagles Medium (DMEM-D5671) (both from Sigma-Aldrich, Steinheim, Germany). Both mediums were supplemented with 10% Foetal Bovine Serum (FBS), 2% L-glutamine, 100 units/ml penicillin and 100 /ml streptomycin (all from Sigma-Aldrich, Steinheim, Germany). Cells were cultured with their respective mediums as a monolayer in 75cm² standard tissue flasks (NUNC, Roskilde, Denmark), kept in a humidified incubator at 37°C with 5% carbon dioxide ($CO_2$), 95 % air and seeded until 75% confluence before the medium was changed. The standard cell culture work was performed with trypsin, Dulbecco´s Phosphate Buffered-saline (PBS) and culture media (all from Sigma-Aldrich, Steinheim, Germany) on a

laminar flow bench with a high efficiency particulate air (HEPA) filter in a sterile environment.

## 3.2 Animal models

A total of 24 female Balb/c (Taconic Biosciences, Ejby, Danmark) mice with an initial weight ranging from 18 to 27 grams were used as model for the 4T1 and 4T1-L cell line.

A total of 12 female non-obese diabetic/severe combined immunodeficient gamma (nod/scid) mice (Jackson Laboratory, Bar Harbour, ME, USA) were used as a model for MDA-231 human mammary cancer cell line. Their weight ranged from 21 to 24 grams.

All experiments were performed when the mice were approximately 6-8 weeks old.

All mice were housed in intraventilated cages (maximum 5 in each) (Makrolon IV, Techniplast Gazzada, S.a.r.l., Buggigiate, Italia) with a room temperature of 21° degrees and air humidity held between 40-60% at the animal facility at University of Bergen. The mice were exposed to a light/dark cycle at 12/12 hours. They had a fixed diet consisting of pellets (Special Diet Service, Witham Essex) and water. The mice were identified by having their tails labeled with a permanent marker.

All experiments with animals in this study were performed in accordance with the Norwegian Animal Research Authority and approved by the local ethical committee (project nr. 20157368). The number of animals was minimized to comply with the ethical committee guidelines.

## 3.3 Anesthesia

All mice were anesthetized with Isoflurane (Isobal®Vet, Orion Pharma Animal Health, Finland) combined with nitrogen oxide ($N_2O$) (1 l/min) and oxygen ($O_2$) (1 l/min) gas

during all cell injections and tumor size measurements. During gas-anesthesia the mouse was placed in a plexiglas chamber flushed with anesthetic gas at a rate of 5 l/min. When the mouse was satisfactory anesthetized the dose was reduced to 2 L/min. The mouse was then placed on a heating pad which kept the body temperature at 37 ºC ± 0.5 ºC and anesthesia was supplied by a nozzle to the nose and mouth area.

To make sure that the mouse was completely anesthetized, the contraction reflex was tested by pinching the sole of the back foot with a tweezer.

All mice were sacrificed under anesthesia by cervical dislocation (all 4T1-L mice after optical imaging) or by $CO_2$.

## 3.4 Preparation of cells before injection

Using the cell nucleocounter SCC-100 and a nucleocassette (Bergman-Nucleocounter-Chemometec, Allerød, Denmark) the number of cells/mL solution was identified as follows:

All cells from each flask were trypsinized into a single cell suspension. In accordance with the manufacturer's instructions, 200 µl was extracted from the cell suspension and mixed with 200 µl of buffer A and B (Bergman-Nucleocounter-chemotech, Allerød, Denmark). Buffer A is a lysis reagent with a pH of 1.25. It acts by disrupting the plasma membrane, leaving the nuclei susceptible to staining with fluorescent dye and propidium iodide (PI). Buffer B is a stabilizing reagent that raises the pH in order of DNA staining to be as efficient as possible.

The suspension was vortexed (MS2 Minishaker, Apendoorn, Netherlands) directly before being loaded into the nucleocassette. Automatically, the cassette uploads 50 µl of the cell suspension and mixes it with PI. By staining the nuclei of cells, the nucleocounter can calculate the number of cells per ml.

The total amount of cells/ml suspension obtained from the nucleocounter was multiplied by three due to dilution factors caused by reagents A and B. The rest of the cell suspension was centrifuged (Eppendorf Centrifuge 5810 R, Hamburg, Germany) at 990 rounds per minute (rpm), at 10°C for 4 minutes before culture medium was removed from the centrifuged cells. Calculated amount of PBS was added to obtain 5 x $10^5$ cells per 0.15 ml suspension according to this formula:

**Formula 2**: Added PBS

$$\frac{\text{Total amount of cells} * 0{,}15 \text{ ml}}{500000 \text{ cells}}$$

## 3.5 Establishing tumors

Each mouse was injected with 5 X $10^5$ cells, in a 0.15 ml suspension subcutaneously into the lower mammary fat pad at the right side at day 1. At this point, all mice were divided into two groups; control and HBO. The two groups were kept separate throughout the experiment. After 8 days, the 4T1 cell line had formed measurable tumors in all mice (7/7), while only a few tumors from the MDA-231 cell line were noticeable (2/6).

## 3.6 Hyperbaric oxygen treatment

A 27 l cylindrical pressure chamber (Oxycom 250 ARC, Tampere, Finland) with an inner diameter of 25 cm and an inner length of 55 cm was used (Fig. 4).

When undergoing treatment, mice were placed in the pressure chamber. The chamber was locked airtight and $O_2$ concentration was monitored by an oxygen cell. Before each treatment, a flush phase with supply of pure $O_2$ for ~15 minutes was conducted with no increase in pressure. When 98% $O_2$ was reached the chamber was pressurized (compression phase) steadily to 2.5 bar for 10-15 minutes. This pressure was maintained for 90 minutes in which the chamber atmosphere was flushed for 5 minutes every 10 minutes to ensure an atmosphere of >97 % $O_2$ at all times. After treatment, the chamber was decompressed slowly to 1 bar over a period of 10 -15 minutes.

Mice undergoing treatment were exposed to HBO from day 7 (4T1 and 4T1-L) or 8 (MDA-231) and every third day until termination of the experiment (day 22 and 33 for 4T1 and 4T1L respectively and day 53 for MDA-231).


**Figure 4**: The hyperbaric oxygen chamber.

## 3.7 Tumor growth measurement

Tumors were measured externally by a caliper immediately following HBO treatment. The tumor shape and approximate size were schematically drawn on day one to ensure proper measurement positions on later measurements (Figure 5).

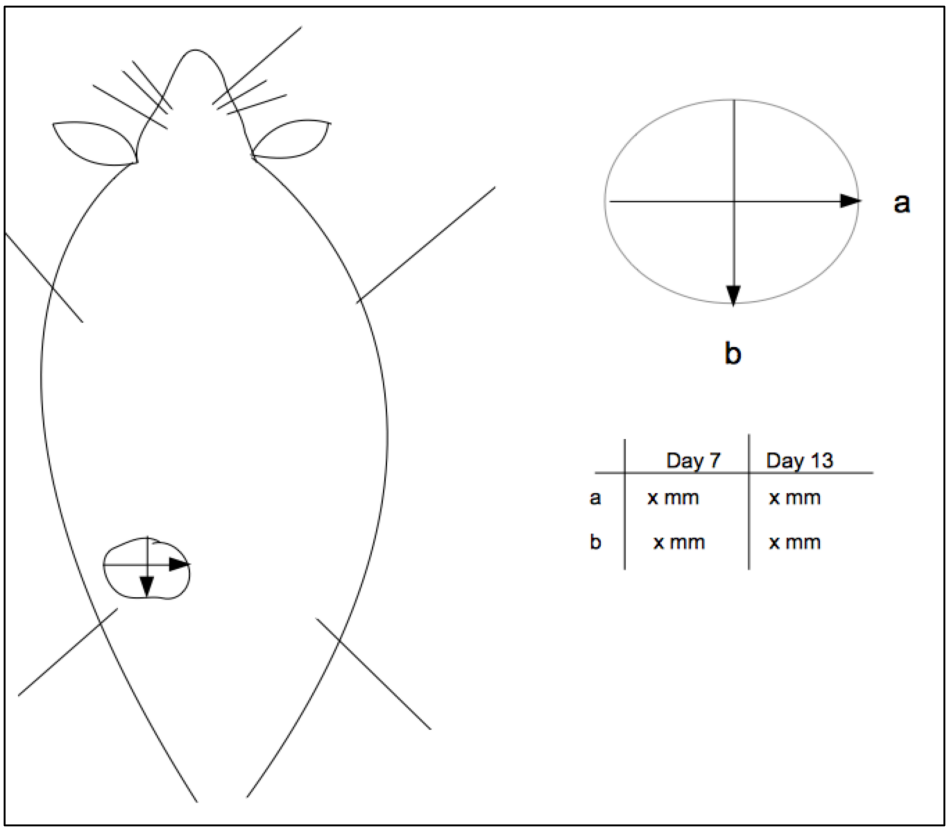


**Figure 5**: Schematic drawing of a mouse with primary mammary tumor used for localization, shape and size measurements.

The tumor was measured bidirectional assuming that the tumor had a cylindrical shape. Tumor volume was estimated according to the formula:

**Formula 3:**

$$\text{Tumor volume } (mm^3) = (\pi/6) \times (a^2) \times (b)$$

- where a is the shortest and b is the longest transversal diameter of the tumor.

All mice were weighed and observed throughout the experiments to get an indication on any substantial health problems.

## 3.8 Optical Molecular Imaging

An optical imager (eXplore Optix™, Advanced Research Technologies Inc., Quebec, Canada) was used to visualize primary tumor tissue and metastasis *in vivo* through the bioluminescent enzyme luciferase present in tumor cells. Mice with 4T1-Luciferase cells were injected intraperitoneally with D-luciferine (150 mg/kg) (Sigma-Aldrich, Steinheim, Germany) diluted in saline (25mg/ml) and anesthetized using isoflurane as mentioned previously (section 3.3). Following ten minutes post injection, the mouse was positioned on its back with extremities fastened to the ground by tape in the optical chamber with a set temperature (35°C). Manual adjustments were set as follows: Integration time: 0.3, region of interest (ROI): Polygon (scanning area was set by manually drawing around the area of interest on the mouse), Scan resolution – 1.5 mm. The intensity value (NC) had to be above 100 or otherwise excluded as background noise. Immediately after acquisition, 2D images were visible. At the experimental endpoint, mice were euthanized by cervical dislocation whilst under anesthesia and primary tumors were immediately removed, snap frozen in liquid nitrogen and weighed. Other organs (lungs, axillary lymph

node, liver, spleen, kidney, primary tumor and bone) were harvested and imaged in a petri-dish with 10% formalin for metastasis evaluation. Finally, organs were prepared for fixation (described in section 3.9).

## 3.9 Isolation of organs/tissues

On the day of termination mice were euthanized (previously described in section 3.3) and the following organs/tissues were dissected out: primary tumor, lungs, axillary lymph node, liver, kidney and bone (part of femur and tibia). The lungs were fixated with 1ml of Bouin´s solution (Gurr BDH Chemicals Ltd., Poole, UK) by cutting the trachea open with a pair of small scissors and injecting the solution into the lungs with a thick needle were the tip was cut off. Lungs were placed in Bouin´s solution for 24 hours and then in 70% ethanol (Sigma-Aldrich, Steinheim, Germany). The ethanol was changed every other day until it became clear and no longer yellow. The tumors were quickly snap frozen in liquid nitrogen and stored in a -80°C freezer (Sdanyo, MDF-C52V) until further use. The bones were placed in 10% ethylenediaminetetraacetic acid (EDTA) solution (pH 7,2) (Sigma-Aldrich, Steinheim, Germany), for decalcification and changed 3 times a week until the bones were soft enough to cut into sections. The rest of the organs were fixated in 10% formalin solution (VWR Chemicals, Leuven, Belgium) for one day. All organs/tissues were kept in 15 or 50 ml Falcon tubes. The samples were delivered to Anne Nyhaug at the Molecular Imaging Center (MIC) at the University of Bergen for paraffin fixation, hematoxylin and eosin (H&E) staining and slicing into 4 µm thick sections. A total of 5-6 sections were taken from each organ at different depths.

## 3.10 Estimation of metastasis

The number of metastases and metastatic area (mm²) on isolated organs were determined by using a light microscope (4 x 10) and camera (Digital Sight, Nikon Corporation, Tokyo, Japan) on paraffin embedded sections stained with hematoxylin and eosin. The software, NIS Elements Confocal 9.0, from Nikon was used. The area of metastases was manually drawn around each cluster of metastatic cells and the program automatically calculated the area (mm²). Due to time limitations, only the lungs and liver were examined for metastasis. For each organ, 4 sections at different depths were chosen for metastasis detection.

## 3.11 Western blot

### 3.11.1 Tissue preparation

Frozen tumors were cut with a scalpel about 2/3 into the middle, and a cross section of tumor tissue (approximately 50 mg) was isolated and kept on ice. Exactly 1ml of denaturing lysis buffer (provided by Tonje Sønstevold, see Appendix A for more details) was added to a tube with homogenizing beads (Bertin Technologies, France).

Tumor pieces were added to the mixture and placed in a tissue homogenizer (Precellys® 24, Bertin Technologies, France) (program 2: 6800 rpm -3x, 10-30 sec.) at 4°C and incubated on ice for 45 minutes. After completion, the samples were visualized to ensure complete lysis of the tumor pieces. The lysate was subtracted and centrifuged at 12000 rpm for 10 minutes at 4°C (Eppendorf 5415R, Hamburg, Germany). The supernatant was collected, aliquoted into 3 x 200 µl samples and stored at -80°C. The pellet was discarded and the beads were washed in lye for reuse.

### 3.11.2 Protein concentration assay

The protein concentration was determined by a Bicinchoninic acid (BCA) protein assay kit, (Pierce™, Thermo Scientific, Rockford, USA) containing reagent A, reagent B and bovine serum albumin standard ampules to establish sample protein concentration.

In order to get the samples to comply with the standard curve, they had to be diluted in double distilled water ($ddH_2O$) (dilution factor 1:50). Five µl of sample were added to 245 µl of $ddH_2O$. Albumin standards were diluted in $ddH_2O$ and prepared as follows: 2 mg/ml, 1 mg/ml, 500 µl /ml, 250 µl /ml, 100 µl /ml, 50 µl /ml and 25 µl /ml. Calculated amount of master mix combining reagent A and B was prepared (ratio 50:1) accordingly:

Number of standards x number of samples x 3 repetitions x 200 µl per well

= Amount of master-mix

To each well on a 96-well plate, 195 µl of master-mix was added. Albumin standards and samples were loaded (5 µl) in triplets (Fig. 6). The plate was incubated at 37°C for 30 minutes and cooled to room temperature.

| | | | | | | | | | | | |
|---|---|---|---|---|---|---|---|---|---|---|---|
| 0 mg/ml | 0 mg/ml | 0 mg/ml | 25 µg/ml | 25 µg/ml | 25 µg/ml | 50 µg/ml | 50 µg/ml | 50 µg/ml | 100 µg/ml | 100 µg/ml | 100 µg/ml |
| 250 µg/ml | 250 µg/ml | 250 µg/ml | 500 µg/ml | 500 µg/ml | 500 µg/ml | 1000 µg/ml | 1000 µg/ml | 1000 µg/ml | 2000 µg/ml | 2000 µg/ml | 2000 µg/ml |
| Sample 1 | Sample 2 | Sample 3 | Sample 4 | Sample 5 | Sample 6 | Sample 7 | Sample 8 | Sample 9 | Sample 10 | Sample 11 | Sample 12 |
| Sample 1 | Sample 2 | Sample 3 | Sample 4 | Sample 5 | Sample 6 | Sample 7 | Sample 8 | Sample 9 | Sample 10 | Sample 11 | Sample 12 |
| Sample 1 | Sample 2 | Sample 3 | Sample 4 | Sample 5 | Sample 6 | Sample 7 | Sample 8 | Sample 9 | Sample 10 | Sample 11 | Sample 12 |
| Sample 13 | Sample 14 | Sample 15 | Sample 16 | Sample 17 | Sample 18 | Sample 19 | Sample 20 | Sample 21 | Sample 22 | Sample 23 | Sample 24 |
| Sample 13 | Sample 14 | Sample 15 | Sample 16 | Sample 17 | Sample 18 | Sample 19 | Sample 20 | Sample 21 | Sample 22 | Sample 23 | Sample 24 |
| Sample 13 | Sample 14 | Sample 15 | Sample 16 | Sample 17 | Sample 18 | Sample 19 | Sample 20 | Sample 21 | Sample 22 | Sample 23 | Sample 24 |

**Figure 6**: Overview over albumin standards and lysate samples on the 96-well plate.

### 3.11.3 Absorbance reading

The absorbance was estimated using a microplate reader spectrophotometer at 562 nm with the software SoftMax® Pro (VersaMax™, Molecular Devices, Sunnyvale, CA, USA). Samples that were obviously not correct (e.g. loading error) were masked. Samples were also checked for severely deviating concentration (optical density) values. A coefficient of variation (CV) value (measure of dispersion) over 10.0 was considered an indication of deviating concentration values that needed to be corrected. Since each sample was loaded three times, we could check if one value deviated significantly from the others, and thus masked. We corrected four and five deviated values from the 4T1 and MDA-231 tumor lysates, respectively.

### 3.11.4 Gel electrophoresis

The protein lysates were selected (control and HBO) and collected from the -80°C freezer and thawed on ice. New 1.5 ml Eppendorf tubes with 30 µl of protein lysate were centrifuged for a few seconds before diluted in 10 µl loading buffer (XT Sample Buffer, Bio-Rad laboratories, California, USA) The proteins were denatured by “boiling” at 95°C for 5 minutes (Dri-Block® DB-2A, Techne, Cambridge, UK) before briefly spun down. The proteins were separated on premade 12% protein gels (Precice™, Thermo Scientific, Rockford, USA) in 500ml of Tris-HEPES-SDS running buffer (BuphJ™, Thermo Scientific, Rockford, USA). The samples were loaded next to a marker (Precision Plus Protein™, Dual Color Standards, Bio-Rad Laboratories, München, Germany) and a normoxic HCC cell lysate (gift from Maria Tveiterås, University of Bergen) as positive control was used in well 12. The samples were added (10 µl) with a control in well 2, HBO in well 3, control in well 4 and so on. The electrophoresis box was connected to an electrophoresis power supply (PowerPack™, Bio-Rad laboratories, CA, USA) and run for 10 minutes at 95 V and 60 minutes at 110 V.

### 3.11.5 Transfer and blocking

The gel with separated proteins was transferred to a membrane using gel transfer stacks (cathode, anode and sponge) in a gel transfer device (all from Invitrogen iBlot™, Life Technologies, Carlsbad, CA, USA) using program p3 for 7 min. Membranes were blocked with I-block buffer (provided by Tonje Sønstevold, University of Bergen, see Appendix A for details) for 1 hour and 30 min at room temperature in order to impede unspecific binding of primary antibody. Thereafter, the membranes were placed in 50 ml Falcon tubes before adding the primary antibody and diluted in I-block to achieve a final volume of 2 ml per tube (see dilution factor for each antibody). Rabbit anti-mouse E-cadherin (ab53033, dilution factor 1:800) and rabbit anti-mouse N-cadherin (ab76057, dilution factor 1:1000) (both purchased from Abcam, Cambridge, UK) were used as

primary antibodies. The tubes containing the membranes, I-block and antibodies were incubated over night at 4°C.

The following day the membranes were washed 3 times x 5 minutes with Tris buffered saline-Tween® (TBS-T) (see Appendix A for more details) to remove unbound primary antibody and to prevent sodium azide ($NaN_3$) in I-block buffer from reacting with peroxidase in the secondary antibody. The membranes were moved from the tubes to small containers together with 10 ml of mixed secondary antibody and TBS-T (dilution factor 1:5000) and incubated for 2 hours at room temperature. Goat anti-rabbit IgG Horse radish peroxidase (HRP) (ab97051, Abcam, Cambridge, UK) was used as secondary antibody.

### 3.11.6 Protein detection

Membranes were washed 2 x 5 minutes with TBS-T and 1 x 5 minutes with 1xTBS (see Appendix A for more details) prior to protein detection. Development of membranes were performed with West Pico Chemiluminescent substrate (SuperSignal®, Thermo Scientific, Rockford, USA) by mixing peroxide solution and luminol enhancer solution with the ratio 1:1. The membranes were put on a plastic cover and the mixture was poured over the membrane with a pipette. The protein bands were visualized (ChemiDoc™ XRS+, Bio-Rad laboratories, CA, USA) and densitometry was performed using the software Image Lab™ for band quantification.

The membranes were reprobed adding rabbit anti-mouse β-actin (ab15263, dilution 1:5000, Abcam, Cambridge, UK) for protein loading control with the procedure as mentioned above.

After development, the visible bands from MDA-231 tumor lysates were quantified into optical intensity values for statistical analyses and comparison between HBO treatment and control group. Due to no observable difference in protein expression we decided not to quantify E- and N-cadherin expression in the 4T1 and 4T1-L tumor lysates.

*Statistics*

For statistical analysis, unpaired two tailed t-test or Wilcox test was used to analyze statistical differences between the two groups. Results were accepted as statistically satisfactory when $p<0.05$. Standard deviations or standard errors of means are indicated in Figures and Tables. The software IBM SPSS 23.0 for Windows was used for statistical analyses, SigmaPlot 9.0 (Systat Software) for creating figures and Image-Lab (from Bio-Rad) for band quantification in western blots.

# 4. Results

## 4.1 Tumor growth

The average 4T1 tumor volume showed unexpectedly, no significant difference between the HBO-treated and non-treated (control) group, neither at day 7 ($p<0.13$) or at day 22 ($p<0.82$). The HBO-treated group measured an average tumor volume of 244±28.5 $mm^3$ at day 7 compared to 171±35.0 $mm^3$ in the control group (Fig. 7). Average tumor volume increased with 815 $mm^3$ in HBO-treated and 921 $mm^3$ in control mice during the course of the experiment.

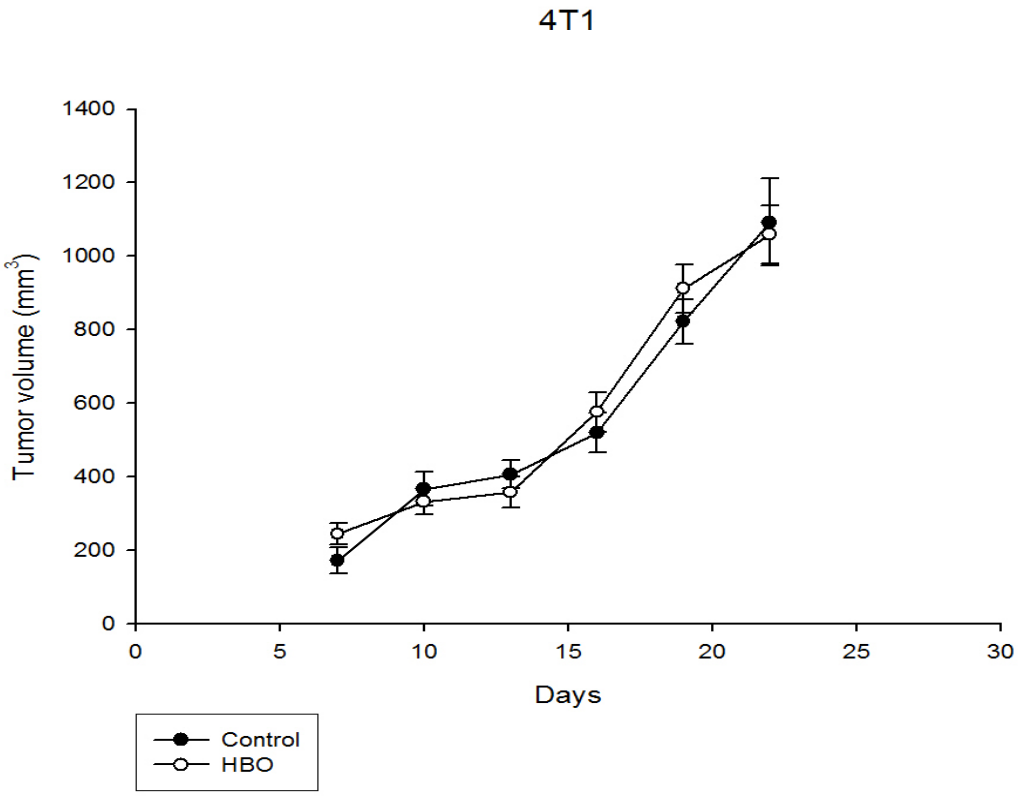


**Figure 7**: The effect of hyperbaric oxygen (HBO) treatment on 4T1 breast tumor growth in treated (n=7) and control (n=7) balb/c mice during a period of 22 days. Mice were treated with 2,5 bar pure oxygen for 90 minutes, every third day. Data are represented as mean ± SEM.

The average 4T1-L tumor volume was significantly lower in HBO-treated compared to controls at day 16 ($p<0.04$), day 19 ($p<0.02$) and the last day ($p<0.04$). The HBO-treated group measured an average tumor volume of 120±10.5 $mm^3$ at day 7 compared to 198±66.1 $mm^3$ in the control group (Fig. 8). Average tumor volume increased with 419 $mm^3$ in HBO and 878 $mm^3$ in controls during the following 24 days.

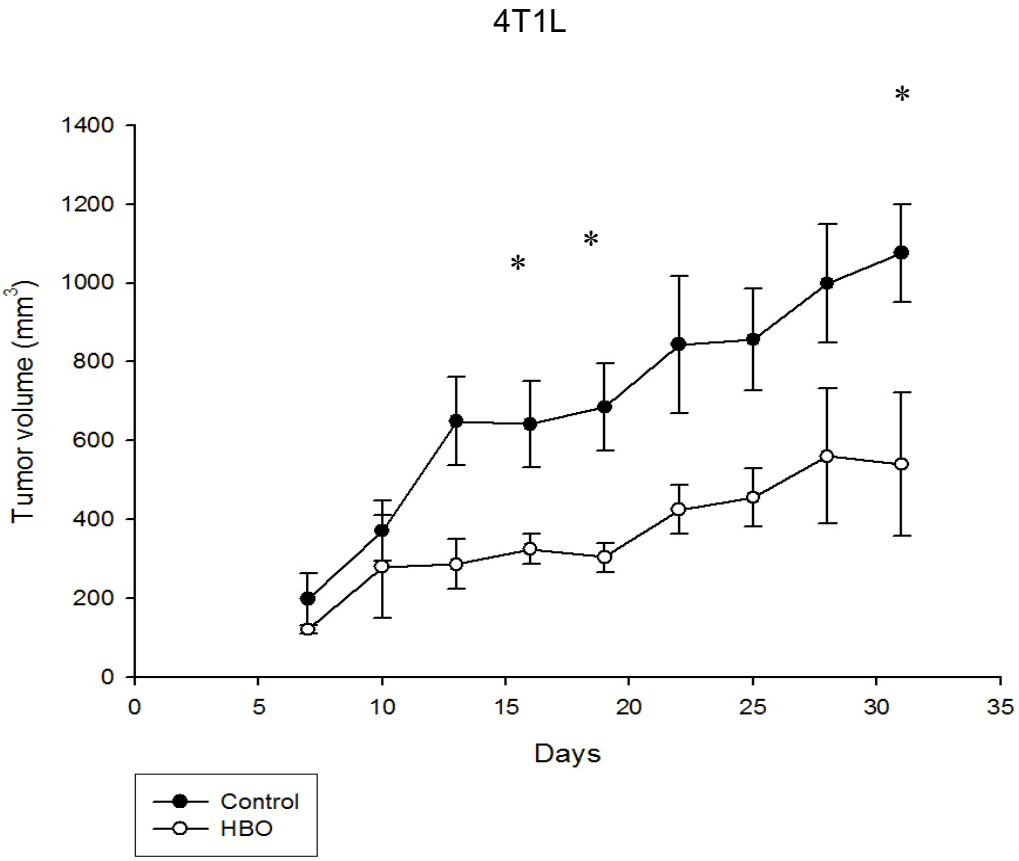


**Figure 8**: The effect of hyperbaric oxygen (HBO) treatment on 4T1-Luciferase breast tumor growth in treated (n=5) and control (n=5) balb/c mice during a period of 33 days. Mice were treated with 2,5 bar pure oxygen for 90 minutes, every third day. Data are represented as mean ± SEM. *p<0.02-0.04.

The average MDA-231 tumor volume was significantly lower in HBO-treated compared to control nod/scid mice at day 30 ($p<0.002$), and day 37 ($p<0.012$), but not at day 53 ($p<0.15$). The HBO treated group measured an average tumor volume of 63.9±12.3 $mm^3$ at day 30 compared to 160.3±20.4 $mm^3$ in control mice (Fig. 9). Average tumor volume increased with 397 $mm^3$ in HBO and 532.3 $mm^3$ in controls during the following 23 days. Tumors (n=12) were measured from day 8, however, due to the low number of measurable tumors, only the tumor volume from day 30 were included in the statistical analysis.

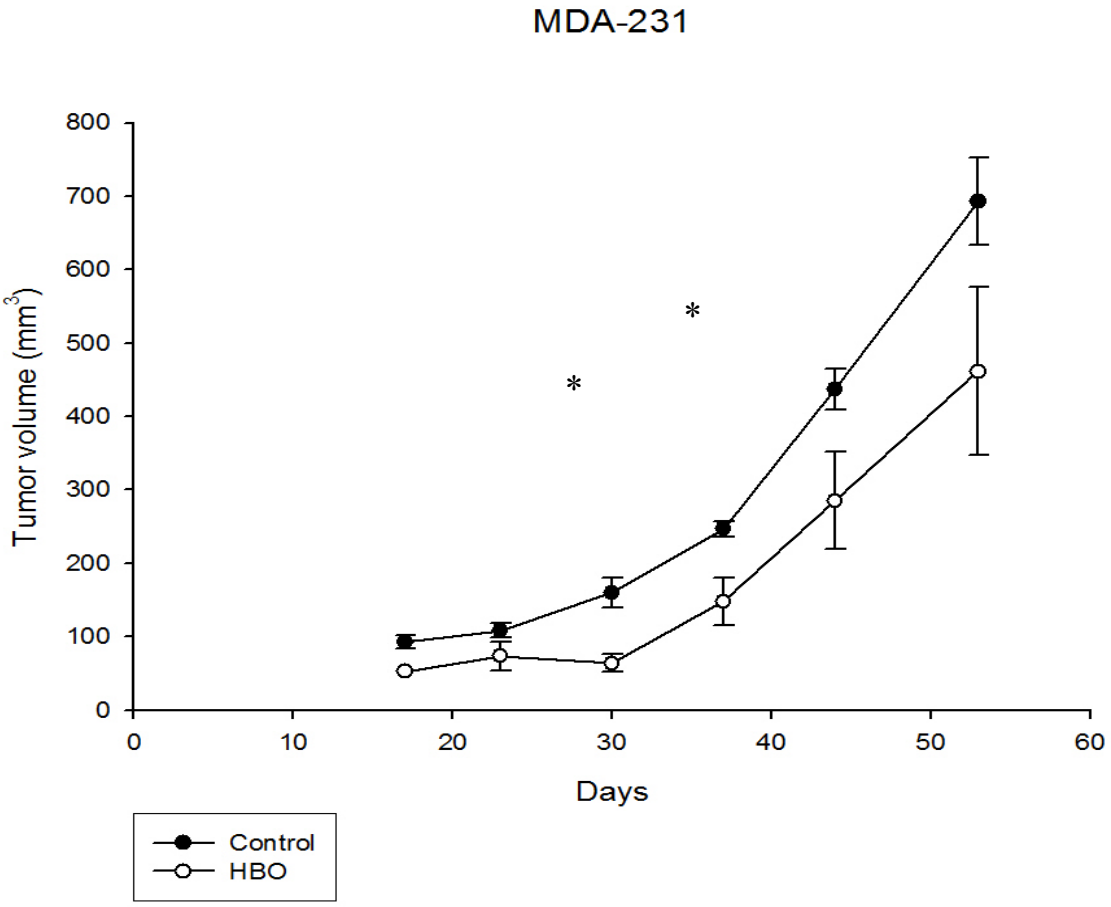


**Figure 9**: The effect of hyperbaric oxygen (HBO) treatment on MDA-231 breast tumor growth in treated (n=6) and control (n=6) nod/scid mice during a period of 53 days. Mice were treated with 2,5 bar pure oxygen for 90 minutes, every third day. Data are represented as mean ± SEM. *p<0.012-0.002)

## 4.2 Metastasis

Macroscopic surface metastases were found in the lungs of all tumor models (Fig. 10). However, due to unfamiliar appearance and resemblance to lymphocyte tissue, we had a slight difficulty determining 4T1-L metastases.

**Figure 10**: A representative picture demonstrating 4T1 surface metastases in the lung is shown.

Paraffin-embedded, H&E stained 4T1, 4T1-L and MDA-231 sections of various organs were used for metastasis number and area estimation. Histological examination of 4T1, 4T1-L and MDA-231 stained sections showed metastasis in the lungs, but not in the liver.

### 4.2.1 Lung metastasis

The 4T1 tumor model showed no statistical difference in the number ($p<0.27$) and area ($p<0.4$) of lung metastases between the HBO-treated and control group. Only 5 out of 7 HBO-treated cases developed metastases, and 4 out of 6 of the controls displayed metastases in the lungs. One of the control mice (mouse nr. 4) had to be sacrificed at day 13 for ethical reasons due to severe tumor growth.

The average area of 4T1 metastases observed in the HBO-treated group was 6.3±3.5 $mm^2$ compared to 8.4±10.2 $mm^2$ for the control group (Fig. 11). The high standard deviation values can be explained by severely deviating values in the metastatic area among mice.

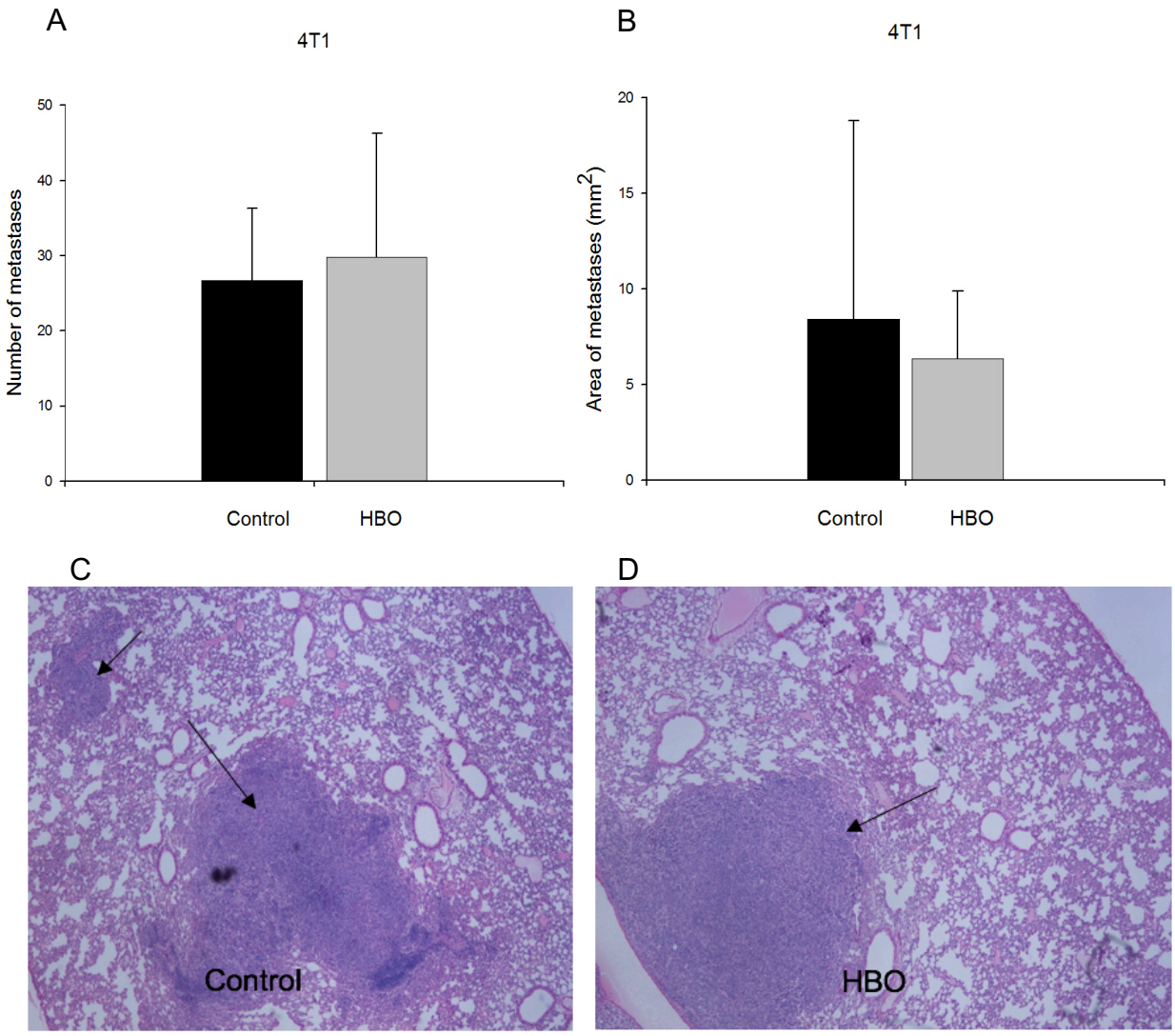


**Figure 11**: The effect of hyperbaric oxygen (HBO) treatment on the metastatic potential of 4T1 tumor cells *in vivo* after 22 days. Histomorphometric quantification of metastasis number (A) and area (B) in H&E stained lung sections in treated (n=5) and control (n=4) balb/c mice are shown. Data are represented as Mean ± SD. A representative lung section in a control (C) and HBO-treated (D) is shown.

The 4T1-L tumor model showed a significant lower area ($p<0.05$) but not number ($p<0.6$) of metastases in the HBO-treated compared to control group. The average area and number of 4T1-L lung metastases were 1.3±0.4 $mm^2$ and 54.0±10.2 in HBO compared to 3.8±1.97 $mm^2$ and 44.7±25.4 in control group, respectively (Fig. 12).

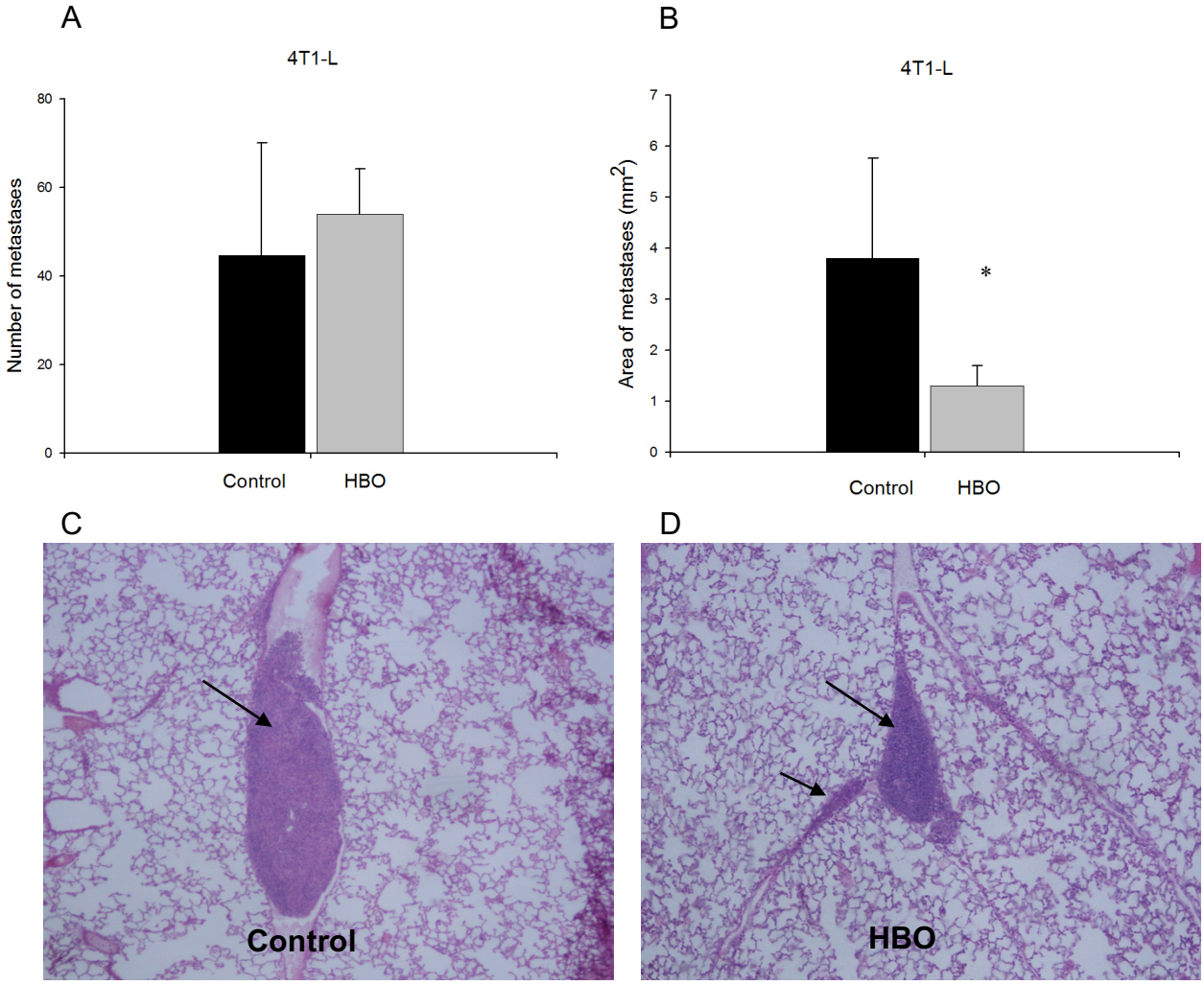


**Figure 12**: The effect of hyperbaric oxygen (HBO) treatment on the metastatic potential of 4T1-L tumor cells *in vivo* after 25 days. Histomorphometric quantification of metastasis number (A) and area (B) in H&E stained lung sections in treated (n=5) and control (n=5) balb/c mice are shown. Data are represented as mean ± SD. *$p<0.05$. A representative lung section in a control (C) and HBO (D) is shown.

The MDA-231 tumor model showed a significant lower number ($p<0.04$) and area ($p<0.02$) of metastases in the HBO-treated compared to control group. The average number and area of observed MDA-231 lung metastases were 107±95 and 0.5±0.6 $mm^2$ in HBO compared to 273±142 and 9.5±13.6 $mm^2$ in control group, respectively (Fig. 13).

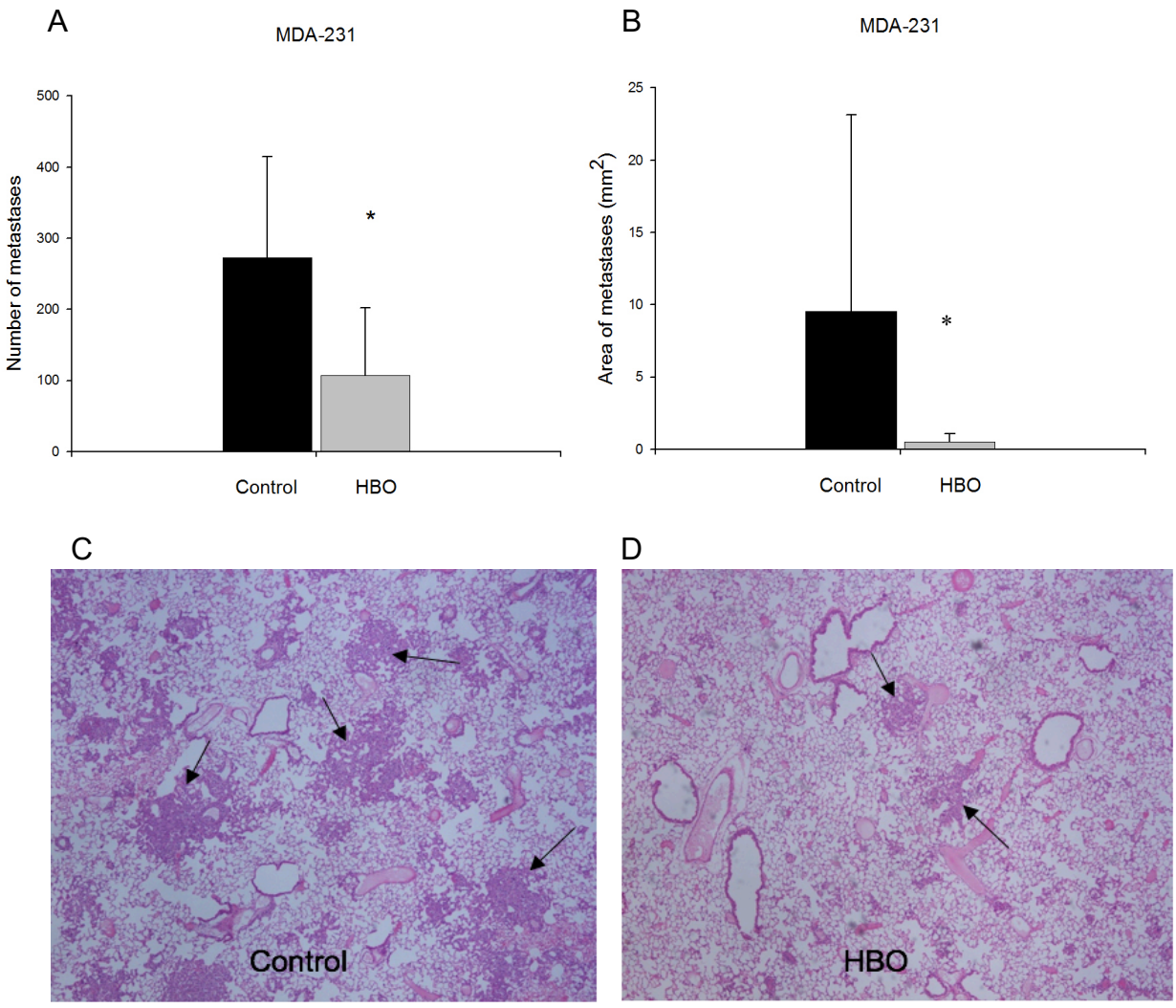


**Figure 13:** The effect of hyperbaric oxygen (HBO) treatment on the metastatic potential of MDA-231 tumor cells *in vivo* after 53 days. Histomorphometric quantification of metastasis number (A) and area (B) in H&E stained lung sections in treated (n=5) and control (n=4) balb/c mice are shown. Data are represented as mean ± SD. *$p<0.05$. A representative lung section in a control (C) and HBO-treated (D) is shown.

## 4.3 *In vivo* optical imaging

Bioluminescent 2D-images showed that the 4T1-L primary tumors of HBO-treated mice were significantly smaller as also indicated by tumor volume and weight at the last day (day 33). We were unfortunately unable to observe any metastases to distant organs, neither *in situ* (Fig. 14) or after imaging the organs separately. This is contrary to the numerous metastases observed in the lungs after H&E staining (as mentioned above).

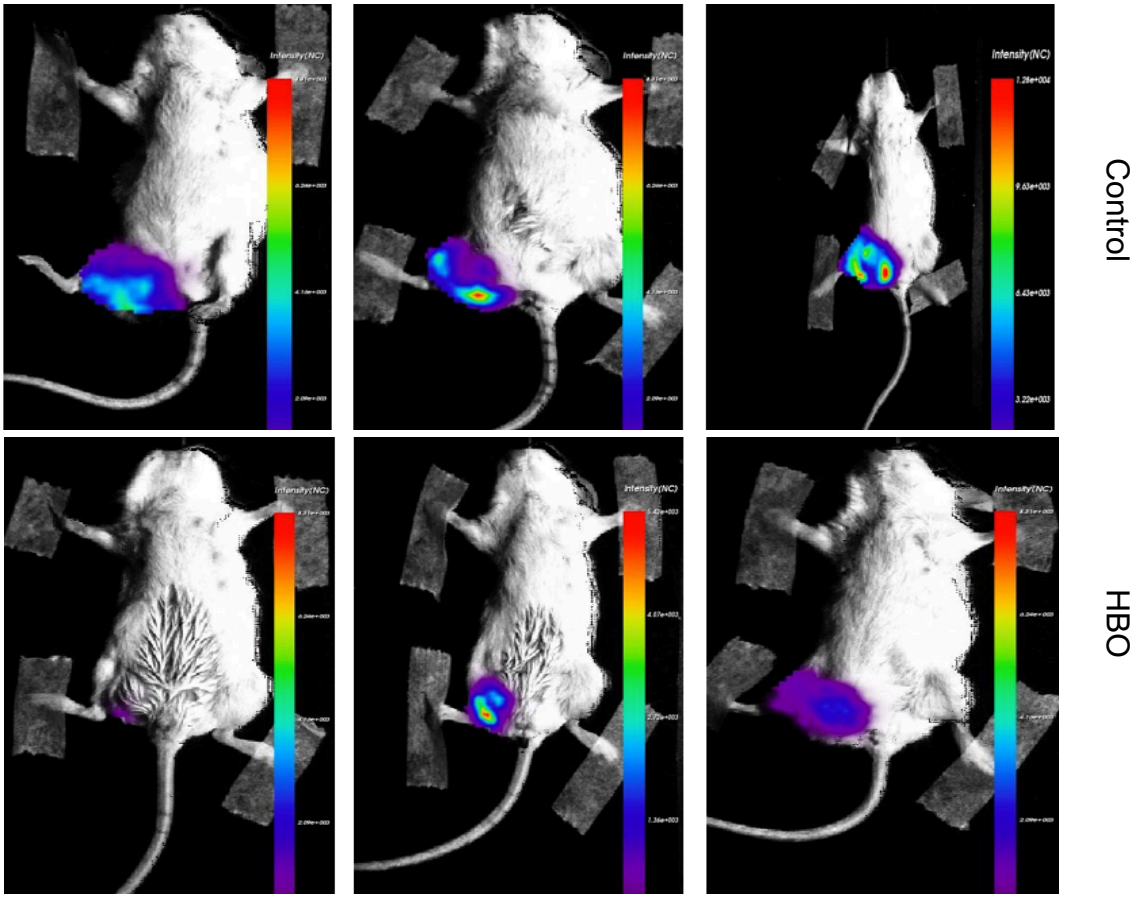


**Figure 14**: *In vivo* optical images of bioluminescent 4T1-Luciferase tumor cells after hyperbaric oxygen (HBO) treatment (control- upper panel, HBO- lower panel) in balb/c mice after 33 days. The relationship between color and light intensity (NC) was calibrated to 8.31 x $10^3$ in all images.

## 4.4 Protein detection

Western blotting was performed using primary tumors to detect levels of N-cadherin and E-cadherin expression. Immunoblots from 4T1 and 4T1-L tumor lysates showed no difference in E- and N-cadherin expression.

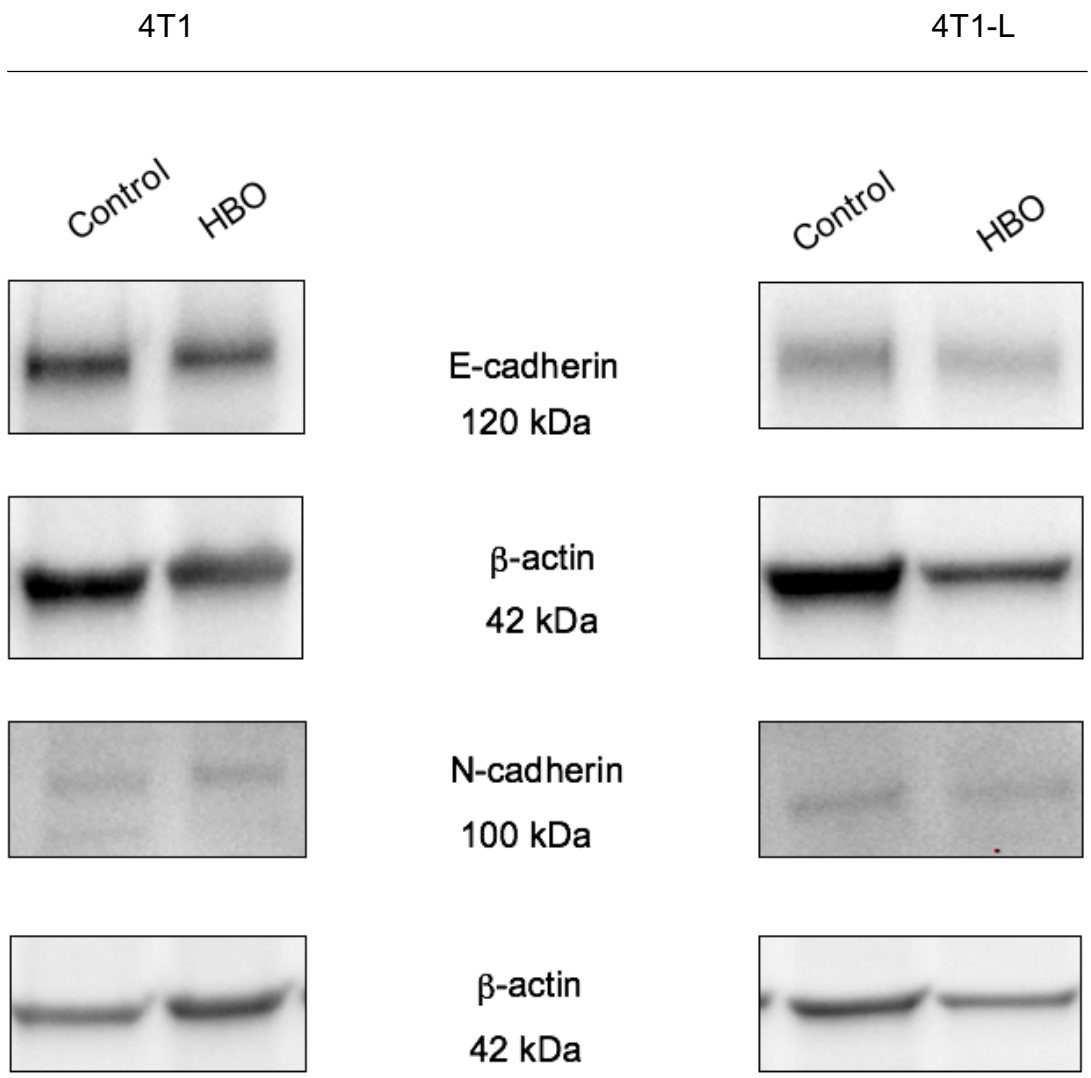


**Figure 15**: E-cadherin (A) and N-cadherin (C) expression is unchanged in western blots of 4T1 (n=5) and 4T1-L (n=5) primary tumors after HBO treatment compared to control, showed by one representative immunoblot.

Immunoblots from MDA-231 tumor lysates indicated a downregulated N-cadherin expression in HBO-treated tumors. However, no expression differences in E-cadherin between the two groups were observed. The downregulated N-cadherin in HBO-treated tumors was confirmed by volume density data and statistical analyses showed a significant difference ($p<0.021$) (Fig.16).

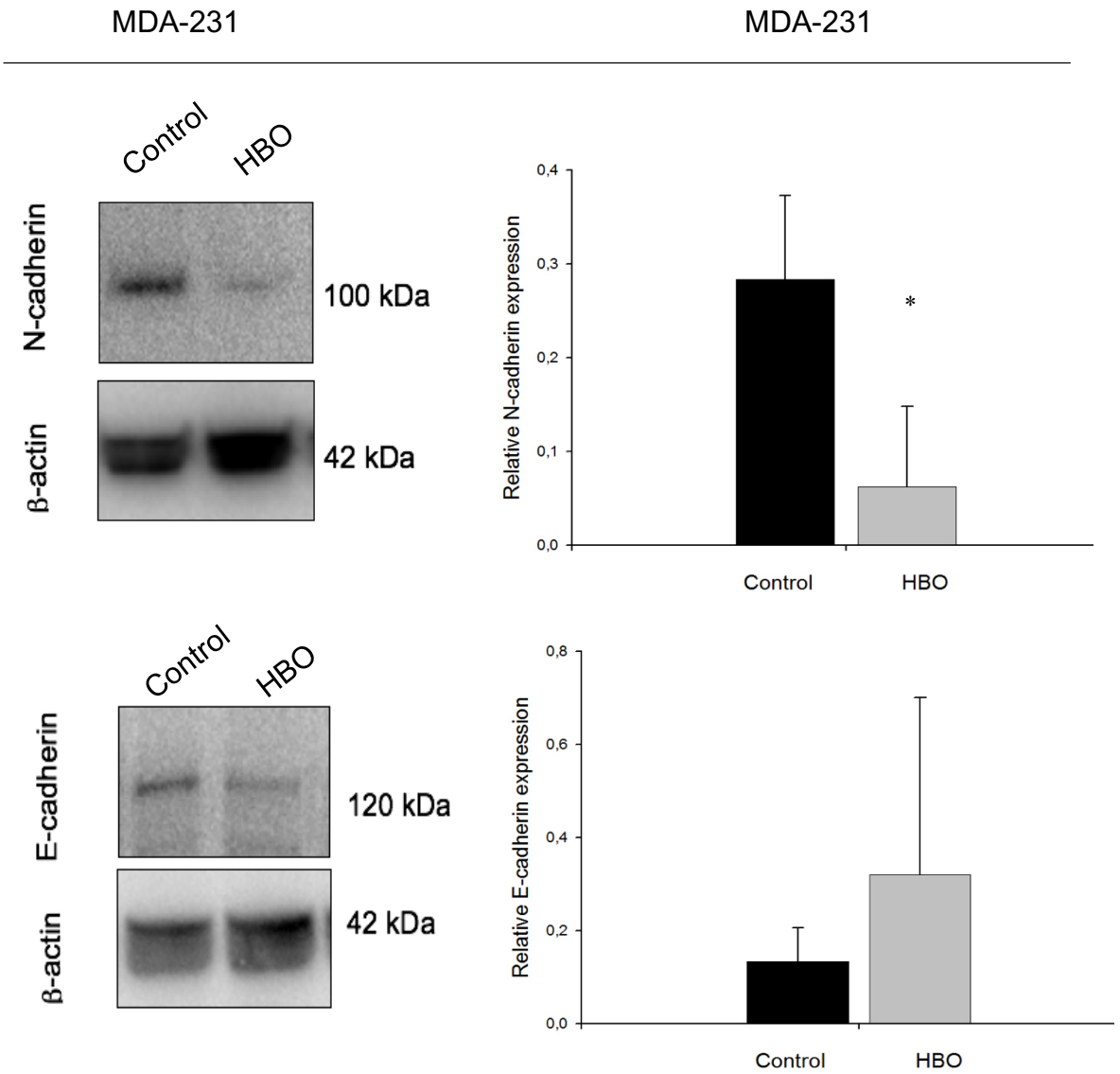


**Figure 16**: MDA-231 tumors constitutively express E-cadherin (A) and N-cadherin (C) in western blot lysates in both groups. The expression of E-cadherin (B) and N-cadherin (D) when adjusted according to loading control (β-Actin) in control (n=5) and HBO-treated (n=5) is also shown. Data are represented as mean ± SD.*$p>0.05$

# 5. Discussion

The strengths and potential weaknesses of the applied methods concerning this study will be discussed in the following section. Thereafter, a general discussion of the results and summarized conclusion will be presented before discussing future perspectives.

## 5.1 Methodological aspects

### 5.1.1 Cell lines

There are several reasons why the murine 4T1 and the human MDA-231 cell lines were chosen for this study. First of all, they are both easily injected into the murine mammary gland, being the anatomically correct site for a primary tumor to develop (orthotopic site) (77, 78). The mammary gland is also the favorable growth site due to appropriate dissemination and expression of the metastatic phenotype (79). Both cell lines are highly aggressive and do metastasize.

However, it is worth mentioning that metastatic dissemination occurs via the hematogenous route as opposed to the initial spread to local lymph nodes via the lymphatic system in human breast cancer (79). Nevertheless, both cell lines metastasize to the same sites as it would in human breast cancer.

The use of 4T1 cells have increased recently because of the high tendency to spontaneously metastasize from the primary tumor multiple distant sites as it would in human breast cancer (77). Due to unexpected tumor growth and metastatic results from the 4T1 tumor growth experiments (discussion below), the use of luminescent 4T1-L cells was implemented. There was not enough time to investigate all organs for metastasis and by using this model we were able to visualize tumor growth and potential

metastases much quicker.

The use of human tumor cell lines is however generally more desirable. Richmond *et al.* (80) stated that: “If one wants to know whether a patient’s tumor will respond to a specific therapeutic regime, one must examine the response of that human tumor, not a mouse tumor”. Human breast tumor cells have previously shown to have a slow tumor take rate and poorly replicate the metastatic process mice (81). However, the MDA-231 xenograft models have shown to display an aggressive phenotype and reliably form distant metastatic tumors even when injected into the orthotopic site (78). We believe that both cell lines serve as excellent models for studying TNBC behavior.

The 4T1 cells were cultured in RPMI-1640 media supplemented with FBS, L-glutamine, penicillin and streptomycin to achieve optimal growth conditions. This combination is commonly used for 4T1 cells in research (74, 82). The MDA-231 cells were cultured in DMEM medium also supplemented with FBS, L-glutamine, penicillin and streptomycin for optimal growth conditions which is supported by literature (82).

The number of cells injected were determined by previous pilot studies performed by our research group, and by previous literature (83). We concluded that $5 \times 10^5$ cells were adequate for inducing primary tumor growth in an ethical perspective for a time frame long enough for metastasis to occur.

### 5.1.2 Animals

While no single animal model can recapitulate all the human cellular and molecular complexities in cancer, a tremendous gain in elucidating breast tumor progression is due to mouse models. Furthermore, tumor-host interactions are complex and not possible to investigate using *in vitro* studies. As previously mentioned, understanding the metastatic process and metastatic sites from a clinical standpoint is paramount since most cancer-related deaths are caused by metastasis and over 30% of patients initially diagnosed at

an early stage will develop metastatic tumors at some point (26). Creating tumor models in animals mimicking human breast cancer behavior as similar as possible expands that understanding and improve treatment options without potentially putting human patients at risk. Mice are advantageous in research due to anatomical and physiological similarities to humans and they can be bread in large quantities in a short matter of time. They are cheap, easy to breed and handle, they don't require too much space and are usually genetically homogenous. Mouse models are also used for predicting efficacy and toxicities of cancer therapeutics before clinical trials (79).

4T1 cells are originally derived from a spontaneous murine mammary tumor of a balb/c mouse and therefore grow rapidly when injected into the fat pad of a syngeneic animal (74). Establishment of 4T1 tumor allografts in balb/c mice has been widely used in research and supported by literature (76, 77, 82).

MDA-231 cells were originally derived by pleural effusion from a breast cancer patient (75) and only immunodeficient mice will not reject the foreign material. Nod/scid mice are deficient in T- and B- lymphocytes as well as NK cells and thus avoid developing an immune response to human cells, like MDA-231. Previously, human tumor cells have replicated and metastasized poorly in mice, making it difficult to study human breast cancer behavior (81). Studies have been dependent on subcutaneous and tail vein injection of cells to achieve tumorigenesis, and hence, mimicking of human tumor progression and metastasis in an adequate way was not possible (81, 84). In addition, when injected orthotopically the primary tumor had to be surgically removed when grown to a considerable size and at that point, several complications arose (84). Nevertheless, the more severely immunocompromised nod/scid mouse have been successfully used to study human breast cancer metastasis, when injected orthotopically without removing the primary tumor (78).

Some researchers state that murine tumor models are the optimal model system for studying malignant progression and responses to cancer therapeutics because they metastasize more effectively and highlight the importance of the microenvironment and

tumor-host interaction (76). Others emphasize the importance of human cancer cells in clinical research to obtain reliable results (80).

Other focuses in animal models have been on understanding the tumor-stroma relationship. Stromal cells and the extracellular environment impact tumor growth, vascularization and the metastatic potential. Murine tumor cell models often display a more aggressive phenotype similar to the behavior in cancer patients. Given the importance of the tumor microenvironment, syngeneic models such as the 4T1 model allow interactions between a normal immune function and tumor behavior (76). As the stroma between the two mouse models differ from each other, tumor progression and development could also differ. Nod/scid mice lack a functional immune system and thus present difficulties in analyzing the effects of stroma on tumor cell growth.

We believe that combining murine and human tumor models in mice for studying human breast cancer is the optimal way of obtaining reliable results.

It is important to know that human and mouse tumorigenesis differ in response to some physiological aspects. They are much smaller, grow quicker and the kinetics of carcinogenesis and the final size of the tumor will be markedly different. Many cell-intrinsic features, gene expressions and immune functions will also differ to some extent (85).

### 5.1.3 Anesthesia

In this experiment, Isoflurane combined with $N_2O$ and $O_2$ gas was used. Gas anesthesia is the preferred option when sedating animals and is commonly used among veterinarians. Gas anesthesia was used in the experimental protocols because the experimental procedure didn't require much time and the animals recovered quickly from the anesthesia.

Isoflurane has been indicated to interfere with the vascular system and decreases blood pressure as well as increase heart rate. However, a low dose of 2 l/minute was used in this study and this is not believed to affect the outcome of the results. Because it is a vasodilator, central body temperature generally decreases, hence the use of a heating mat maintaining the body temperature of the mice at approximately 37°C throughout the procedure.

### 5.1.4 Tumor growth

Tumor growth was assessed by estimating the tumor volume using a caliper and a standard formula. This procedure is not optimal since only measuring the tumor externally will not generate an exact volume. This is because the surrounding skin will always be implemented. To accurately measure the volume, the tumor has to be dissected out, and this can only be performed at the end of the experiment eliminating the ability to follow growth over time. The tumors were dissected out and weighed at the last day to compare with our growth measurements. However, it was impossible to remove the whole primary tumor due to local infiltration and tendency for cells to invade the limb area. Therefore, this was not a better option when using these invasive tumor models.

By using the caliper method, we are also able to compare results with previous studies at our laboratory. All tumors are also measured in the same manner, making any differences between the groups apparent. In addition, some claim that this method is subjective and difficult to accurately reproduce. To justify this, all measurements in the present study were performed by the same operator and by not looking at the previous measurements, any irregularities would affect both experimental groups equally. Thus, any subjective inaccurate measurements would still generate acceptable results.

The tumors differed somewhat in shape, which could affect the results because the

formula assumed all tumors had a cylindrical shape. Again, this applied to tumors in both experimental groups and any differences would therefore be equally measured. Both 4T1 and MDA-231 tumors displayed varied differences in size in both HBO and control groups. Since accurate number of cells was injected into the same site under equal conditions, the reason for this is uncertain.

### 5.1.5 Hyperbaric oxygen treatment

The reasoning for choosing HBO treatment has been described previously (section 1.5). Studies have shown that the reduction in tumor growth was inversely correlated to enhanced oxygen pressure (86). Furthermore, 2 bar HBO exposure lead to induction of MET and changes in metabolism in DMBA-induced breast cancers (57). Recent studies have also investigated the effect of 2.5 bar HBO treatment on genetically engineered 4T1 tumor cells in vivo showing a tumor inhibitory effect (87). Other studies have also reported reduced tumor growth compared to controls from hyperoxic treatment exposures lasting for 90 minutes (73, 87). Since HBO treatment up to 2.5 bar for 90 minutes each exposure is considered safe and clinically relevant, our experimental protocol included administration of HBO at 2.5 bar to potentiate the beneficial effects on tumor progression and metastasis.

Toxic effects of hyperoxia have been observed in the central nervous system and lungs at doses above 2.5 bar or over daily exposures lasting several weeks. The toxic effects included seizures, visual changes, sweating, muscle twitching, coughing, pulmonary fibrosis and shortness of breath (88). As expected, no symptoms of toxicity could be observed during exposures and the course of the experiment, indicating that the treatment protocol was safe. However, insufficient inner ear equilibration from compression and decompression could cause unpleasantness and even more serious side effects. Thus in the present study, both compression and decompression was performed slowly allowing time to equilibrate. Some mice did however, scratch their ears

and shook their heads during the pressure changes indicating a slight discomfort. Decompression/compression was then slowed down even more until they started behaving normally.

There is a small risk of developing fire in a pure oxygen atmosphere and adequate precautions such as keeping the chamber litter- and oil-free was therefore undertaken.

### 5.1.6 In vivo optical imaging

Bioluminescent-based optical imaging was chosen for this study due to the ease and non-invasive monitoring of cancer progression in animal models. Due to the unexpected tumor growth results from 4T1, we wanted to implement 4T1-L cells to possibly uncover any metastases *in vivo* in addition to evaluate the response of another 4T1 tumor model. Another huge benefit of this method is the continuous analysis of changes in tumor progression over time without sacrificing the animals (85). This new approach is widely used instead of autoflourescent-based imaging because external excitation from tissues are avoided leading to background-free imaging conditions (89).

The luciferase-expressed tumor cells (4T1-L) catalyze the oxidation of luciferin (injected 10 minutes prior to imaging) to oxyluciferins and yellow-green light photons are released in the emission spectrum (530-640 nm) (90). The reaction was recently estimated to only produce a 40% quantum yield, yet sufficient enough to produce a detectable light (91). There are several other bioluminescent reporter proteins, all with advantages and disadvantages. The firefly luciferase and D-luciferin substrate have a high sensitivity and low signal-to-noise ratio. There is also a quantitative correlation between signal strength and signal numbers and different colors allow multi-component monitoring. However, it requires exogenous luciferin injection and fast consumption of luciferin can lead to an unstable signal

There are some constrains to visualize and perform data collection from a living model.

The optical properties within a biological tissue sample are dependent on several factors. The location and number of functional luciferase cells and the flux of photons from them within the sample will somewhat differ and impact the final image (92). Nevertheless, scattering and bioluminescent absorption can be reduced by increasing the wavelength which allows us to measure greater amounts of signal intensity (89).

The route of substrate (D-luciferin) injection should also be considered because it can have influential effects on the bioluminescent signal. Intraperitoneal injection was chosen for this study as it is convenient and widely used in this kind of research. However, D-luciferin must absorb across the peritoneum to reach the luciferin-expressed tumor cells. Absorption rate can vary and lead to luminescent signal variations, thus impacting the reproducibility of the results. Intravenous injection of D-luciferin has shown to offer better repeatability and sensitivity than intraperitoneal injection in small tumors (93). Operator error can also include unintentional injection into the bowel which produces a low or undetectable signal. Intraperitoneal injection also produces a lower signal than subcutaneous injection in subcutaneous tumors, but it can also over-estimate tumor size localized intraperitoneally due to the direct contact of D-luciferin and luciferase-expressed tumor cells (94). One must therefore carefully select the appropriate route of injection depending on the location and type of tumor cells inside the animal. For subcutaneously grown breast cancers, we believe that intraperitoneal injection with D-luciferin was the appropriate method.

### 5.1.7 Histological quantification

The other method of evaluating metastasis in different tissues was to stain paraffin-embedded sections of organs and tissues with H&E and assess number and area of metastases under a light microscope. This method is very time consuming, and as only 4-5 sections were used, the whole organ could not be assessed. It does however, provide equal assessment amongst all samples and it is easy to reproduce. Manual

counting and outlining metastases could potentially deviate from specific actual values however, the same investigator was used to assess all samples in this study to assure equal measurements.

In this experiment, metastasized tumor cells could easily be distinguished from normal cells in lung sections from MDA-231 and 4T1 tumor models which leaved less room for speculation and inaccurate results. However, the 4T1-L tumor model was more difficult to assess. The metastatic lesions were not easily distinguished from normal tissue and infiltrated lymphatic tissue, thus realistic quantification of metastases could not be assured.

### 5.1.8 Western Blot

Western blot is a widely established and used method for protein detection and quantification in research. Although numerous errors in the lab could arise in this multi-step process, the results are highly valuable and appreciated in many areas of science. Recent advances in technology provide equipment that leads to faster and easier ways of performing western blotting as well as improving results.

In this study, we initially tried lysating the tumor tissue with the newly developed Bioruptur machine (Biorupture®Pico, Diagenode, Seraing, Belgium) because it lyses both tissues and cells. Unfortunately, we had to use 12-15 cycles (significantly more than the manual suggested) before complete tissue lysis and our results yielded very low signals. Our hypothesis is that the epitope for E-cadherin and N-cadherin were destroyed by this method. We also predicted that this could occur if we used a sonicator, so only the centrifuge was used in the end for tissue lysis.

We observed a markedly different loading concentration in β-actin, and even though adjustments for this difference through densitometry was performed, the optimal way would have been to repeat the process and adjust for protein concentrations.

## 5.2 Results

The present study showed reduced primary tumor growth and reduced metastatic effect of HBO treatment in triple negative human (MDA-231) and murine (4T1-L) breast tumor models in *in vivo*. Further, the EMT marker, N-cadherin was significantly downregulated by HBO treatment in the MDA-231 xenograft. There seemed to be an insignificant effect on tumor growth and metastasis in the murine (4T1) allograft.

### 5.2.1 Tumor growth estimation

Because hypoxia is a common feature in tumors and generally accepted as a promoter of aggressive tumor growth and metastatic potential, we wanted to target the hypoxic tumor microenvironment. This was conducted by investigating the effect of enhanced tissue oxygenation by HBO treatment in murine and human breast tumor models.

*4T1 and 4T1-L*

The present study showed no significant difference in 4T1 primary tumor growth between treated and control, indicating that 2.5 bar HBO exposure did not effectively reduce tumor growth. This is not in agreement with previous studies showing reduced tumor growth found in 4T1 and chemically induced breast tumor models in response to HBO treatment (57, 86, 87, 95). In fact, DMBA-induced tumor growth seemed to be dose dependent and 2.0 bar HBO exposure lead to a smaller tumor size than initially at day 1 (57). It is worth mentioning however, that DMBA-induced tumor models are more heterogeneous and represent endocrine receptor-positive breast cancer which is less aggressive than the TNBC cell type 4T1.

Nevertheless, because the 4T1 tumor growth response to HBO was unexpected due to previous studies at our laboratory (87), we wanted to investigate another 4T1 model

(4T1-L) that in addition could visualize the effects on tumor size and metastasis *in vivo*. There was a significant reduction in tumor growth in response to HBO compared to control in this latter model. This was also in accordance with the *in vivo* images that displayed smaller tumor size in HBO-treated mice. The tumor did not however, shrink as the DMBA-induced tumors did. Because 4T1 cells were obtained from a different provider, there is a possibility that 4T1-L cells behaved differently and were not as aggressive as in accordance with previous research.

The unexpected 4T1 tumor growth response could however, be due to numerous reasons. Perhaps the most reasonable hypothesis is that the 4T1 tumor cells have undergone several mutations and become significantly more aggressive than the once used earlier by our laboratory. The degree of sub-culturing a cell line (passage number) affects the cell´s characteristics such as responses to stimuli, morphology, protein expression and growth rate (96). Although the underlying mechanisms are poorly understood, compelling data of passage-dependent effects on mammalian cell lines has accumulated through these past two decades (96). A study comparing low and high passage number in human prostate cancer cells reported that high passage number correlates to changes in PI3K/Akt pathway, which may have implications in various stages of prostate cancer (97). Hence, cell lines at high passage numbers may develop malignant transformation. It is therefore of interest to ensure low passage number to produce reliable and reproducible results. Since we used passage number 8 and 9 for our present study which is generally not considered “high”, we don’t believe this would have any major effects on the 4T1 cells behavior. However, cells within a cell culture compete for nutrients and cells growing faster, can outgrow other cells. This “survival of the fittest” concept can give rise to transforming cells that do not resemble the original starting material. Contamination from previous improper laboratory work could also influence the cell culture environment and contribute to cell differentiation. Thus, it is of interest to continuously test and examine the cell line of use and compare it to the original type. Due to the unexpected results, this will be performed for this specific set of cells.

Since the hyperbaric chamber has been moved to another location compared to previously mentioned studies, it was of great interest to ensure that the hyperbaric chamber had 100% pure oxygen at the specific flushing and pressurizing protocol we used. Thus, the technicians at our department controlled for this and confirmed that our HBO exposure profile was accurate.

Nevertheless, due to the well documented effects of HBO treatment we can still conclude that it reduces murine breast tumor growth (previous 4T1 studies and the present 4T1-L) and that our results from 4T1 deviate from this conclusion. The reason for the lack of HBO treatment response in the 4T1 model is therefore not elucidated at the present time.

*MDA-231*

Reduced tumor growth was found in the human MDA-231 breast tumor model after HBO treatment compared to controls. All tumors were still significantly larger on the last day compared to day 1. Although research is lacking on the HBO treatment effects on human breast tumors, our results correspond to previous research in chemically induced (DMBA) and murine breast tumor growth (57, 86, 87, 95) Thus, murine and human breast tumor models seem to share a common oxygen dependent inhibitory growth mechanism. The anti-tumor effects of HBO treatment could be pro-apoptotic, anti-proliferative and anti-angiogenic as previously found breast tumor models *in vivo* (57, 86, 87).

### 5.2.2 Metastasis

Since tumor hypoxia is associated with increased metastatic ability as stated in the introduction (52), we hypothesized a reduction in the metastatic potential of tumor cells after HBO treatment. Histological examination of H&E stained sections in the different models was performed to evaluate any possible metastatic effect.

*Metastasis detection*

Macroscopic surface metastases were observed in the lungs of control and HBO-treated mice with MDA-231, 4T1 and 4T1-L primary tumors. The presence of tumor cell metastases in the lungs is in accordance with the findings of Tao *et al.* (76) and Minn *et al. (98)* where 4T1 and MDA-231 lung metastases were visualized by biophotonic imaging. The metastatic potential in the 4T1 tumor model was significantly higher than in MDA-231 model, as to be expected since they are more aggressive. Duration of experiments with 4T1 cells do not normally exceed 30 days due to severe growth of primary tumors in mice. Since 4T1 tumor growth is also more aggressive, one can speculate if there is a correlation between tumor growth aggressiveness and metastatic potential. Interestingly, the possible causality between tumor size and metastatic risk to lungs in breast cancer have been investigated through the previously defined “lung metastasis gene-expression signature” (LMS) study (99). The data indicated that a confirmed LMS in the metastatic tumor confer primary tumor cell growth advantage and hence, tumor growth can be a marker for metastasis.

*HBO and 4T1 and 4T1-L lung metastasis*

The results indicate that HBO treatment did not reduce the metastatic potential of the 4T1 tumor model compared to control. A similar study conducted by our research group also discovered no impact of HBO treatment on the metastatic capability of the 4T1 tumor model over time (100). However, as this was performed with a different HBO protocol and on nod/scid mice, the results may not be totally comparable. Another study observed a significant reduction in large 4T1 tumor colonies in the lungs after intravenous injection *(101).* One could hypothesize that if 4T1 tumor growth was significantly reduced by HBO treatment as in accordance with previous studies (57, 73, 86), the metastatic potential would also be reduced (99). This could also be applied to the 4T1-L model where significantly reduced tumor growth and lower area of metastases were found.

*HBO and MDA-231 lung metastasis*

Interestingly, HBO treatment showed significant effects on reducing the metastatic potential of MDA-231 tumor cells to lungs. Existing research concerning HBO treatment effects on human breast cancer metastasis models is lacking. Therefore, since the MDA-231 cell line is of human origin and represent the most negative prognostic breast cancer type (triple negative), these findings can be of great clinical importance and needs therefore to be studied further.

*Metastatic effect of HBO*

Given that HBO reduces the hypoxic state of tumors, the reduced metastatic potential of tumor cells must be attributed to the effects of enhanced tumor oxygenation. In addition, since low tumor $pO_2$ in patients is associated with increased metastatic potential stated in the introduction (58, 59), certain steps in the metastatic cascade must be hindered by hyperoxia. Since HBO treatment reduces tumor growth, one could also hypothesize reduced metastatic potential. In particular, the reduced tumor cell proliferation, vascular density and increased apoptosis render tumors less aggressive, indicating reduced malignancy. Although research concerning HBO effects on the metastatic cascade is lacking, several studies could not find metastasis induction after HBO treatment in mice with different cancer types (87, 102, 103). Furthermore, Haroon *et al. (101)* observed a significant reduction in large 4T1 tumor colonies in the lungs after intravenous injection indicating that HBO treatment is not prometastatic, but restricts tumor cell growth. The significant reduction in the metastatic ability of human and murine breast tumors after HBO treatment indicates that oxygen might be a contributing factor in metastasis. Furthermore, since HBO treatment has previously shown to induce MET (57) which is believed to counteract the malignant effect of EMT in metastasis progression, this hypothesis is particularly interesting.

*HBO and EMT*

As stated, hypoxia has shown to predispose for tumor metastases through induction of EMT (54, 55). Furthermore, it is well established that highly aggressive epithelial tumors display a change in cadherin expression by an upregulation of N-cadherin and downregulation of E-cadherin (104). Therefore, the major EMT markers, E cadherin and N-cadherin expression in primary tumor lysates was investigated. Our results showed a significant reduction in N-cadherin expression in MDA-231 tumor lysates after treatment compared to controls. E-cadherin expression seemed to be unaffected in the two groups. These results indicate that EMT was affected to some extent by HBO which could be contributing to the reduced metastatic potential of MDA-231 tumor cells. To elucidate whether the effects incused MET, several other expression analyses are needed. However, these results are in accordance with the previous study where induction of MET was mainly characterized by a decrease in N-cadherin and increase in E-cadherin after HBOT (57). As DMBA-tumor models are more heterogenous and could be considered less aggressive than the highly invasive human MDA-231 model, this is particularly promising.

However, the seemingly unaffected expression of E-cadherin remains to be elucidated. Normally, a loss of E-cadherin expression is typically the most representative occurrence in EMT because it is a cell-cell adhesion facilitator (105). In addition, decreased expression of E-cadherin has been seen invasive breast cancers and a recent study reported that EMT and its associated downregulation of E-cadherin is required for the development of metastasis (106). Due to the aggressiveness of the MDA-231 cells compared to the DMBA-induced model, the effects of HBO treatment could have had less impact E-cadherin expression.

On the other hand, highly invasive breast tumors have shown to contain upregulated N-cadherin expression (107). A knockdown of N-cadherin lead to cell increased apoptosis, decreased invasiveness *in vitro* and inhibition of metastatic tumor formation *in vivo* was seen in eosophageal carcinoma (108). In addition, “forced” N-cadherin expression in

transgenic mice containing a mammary tumor promoter lead to increased lung breast tumor cell motility and metastases compared to control (109). Another study found that breast tumor cells “forced” to express N-cadherin did not show a downregulation of E-cadherin but still promoted motility and invasion (110), indicating that N- is dominant over E-cadherin and that its expression alone contributes to malignant progression and therefore not a consequence of it.

Hazan *et al*. (107) reported that N-cadherin promoted breast cancer metastasis through interactions between the breast tumor cells and stromal cells. HBO treatment reduces the hypoxic state of tumors and thus the tumor stroma. One hypothesis could be that the effects of enhanced oxygenation changed the interaction between N-cadherin and stromal cells and lead to reduced expression of N-cadherin, and that E-cadherin expression was more difficult to target by HBO. However, much needs to be elucidated in the mechanisms behind these changes in the tumor microenvironment.

In summary, as N-cadherin plays a direct role in promoting tumor cell motility and invasion, our results are promising in relation to metastasis inhibition regardless of E-cadherin expression.

## 5.3 Conclusion

The overall aim was to target the hypoxic environment.

We have adressed and answered the following specific sub-aims:

**1. Investigate the effect of hyperbaric oxygen treatment on the malignant progression of human (MDA-MB-231) and murine (4T1 and 4T1L) breast tumors *in vivo*.**

- Repeated HBO treatment significantly reduced tumor progression in the human (MDA-231) and murine (4T1-L) breast cancer model without affecting the murine 4T1 model.
- The metastatic ability of human (MDA-231) and murine (4T1-L but not 4T1) tumor cells to lungs were also significantly reduced after HBO treatment.

**2. Visualize tumor size and potential metastases *in vivo* through biophotonic imaging**

- *In vivo* imaging of balb/c mice with primary murine 4T1-L tumors was performed without detecting any metastases to distant sites. Reduced primary tumor size was observed in HBO-treated mice.

**3. Elucidate if hyperbaric oxygen treatment would influence major epithelial to mesenchymal transition markers and thus, the metastatic potential.**

- HBO treatment influenced EMT through downregulation of N-cadherin expression in human (MDA-231) primary tumors. The reduced metastatic potential could possibly be attributed to this downregulation.

## 5.4 Future perspectives

The present study was part of a larger collaboration project and in order to minimize the number of animals, frozen tumors, tumor lysates and organs were stored for later additional analyses.

Future studies should further investigate tumor progression and reduced metastatic potential effect of HBO treatment on different human breast cancer models. In particular, since metastasis is responsible for most cancer-related deaths, any therapy that could reduce the metastatic potential is important.

Factors involved in the development of metastasis should be investigated to better understand the mechanisms behind the metastatic cascade. This would enable successful cancer therapies. As EMT is considered a crucial initial step in metastasis development, additional effectors other than E- and N-cadherin is likely to yield new insights into metastasis. In particular, expression analysis of contributing factors to EMT should be elucidated in order to establish if MET is induced by HBO. The transforming growth factor beta (TGF-β) signaling pathway has been implicated in the several aspects of the metastatic process and is thought to contribute to EMT by inducing E-cadherin.(111). It would be interesting to look at expression of TGF-β in different cell lines to possibly verify that E-cadherin is in fact, downregulated. More importantly, if E-cadherin expression is in fact unaffected by HBO treatment in human breast tumor cells, we could implement TGF-β-knock out mice in HBO treatment. Other inducers of EMT; *TWIST* and *SNAIL* that have shown to correlate with elevated characteristics of breast cancer stem cells (BCSC) contributing to cancer progression (112, 113).

Moreover, the receptor tyrosine kinase Axl is induced by EMT and show enhanced expression in metastatic breast tumors. Enhanced expression is correlated with reduced overall survival in breast cancer patients. More interestingly, a complete prevention of metastasis in highly invasive breast tumors was seen when Axl was knocked out (114). We suggest a further investigation into identification of Axl in response to HBO treatment

as well as targeted treatment of Axl-expressing tumors.

Breast cancer research have identified several useful metastatic markers associated with a poor prognosis  An extensive assessment identified several genes that mediate breast cancer metastasis to the lungs through *in vivo* selection and transcriptomic analyses (98). Interesting genes encoding for the epidermal growth factor family member epiregulin (*EREG*), the MMP collagenase (*MMP1),* the cell adhesion molecule (*SPARC)* and the cell adhesion receptor (*VCAM1).* As they have established a lung metastatic signature in an MDA-231 model, identification of those genes in the primary and metastatic tumor after HBO treatment would be interesting since tumors expressing the signature predict poorer overall survival (98).

Furthermore, the tumor microenvironment has gained special interest due to its contribution of tumor progression and metastasis. As stated in the introduction, the “seed and soil” theory explains the variance between metastatic sites in different cancer types. Investigation into the pre-metastatic niche prior to the development of metastasis could yield new insights into the mechanisms behind the development of this favorable tumor growth environment.

# Reference List


1. Pecorino L. Molecular biology of cancer. Eight ed: Oxford University Press; 2012.
2. National-Cancer-Institute. Tumor Grade 2013 [cited 2016 03.04]. Available from: http://www.cancer.gov/about-cancer/diagnosis-staging/prognosis/tumor-grade-fact-sheet.
3. Hanahan D, Weinberg RA. The hallmarks of cancer. Cell. 2000;100(1):57-70.
4. Hanahan D, Weinberg RA. Hallmarks of cancer: the next generation. Cell. 2011;144(5):646-74.
5. Hanahan D, Folkman J. Patterns and emerging mechanisms of the angiogenic switch during tumorigenesis. Cell. 1996;86(3):353-64.
6. Yang L, Pang Y, Moses HL. TGF-beta and immune cells: an important regulatory axis in the tumor microenvironment and progression. Trends Immunol. 2010;31(6):220-7.
7. Macheda ML, Rogers S, Best JD. Molecular and cellular regulation of glucose transporter (GLUT) proteins in cancer. J Cell Physiol. 2005;202(3):654-62.
8. DeNardo DG, Andreu P, Coussens LM. Interactions between lymphocytes and myeloid cells regulate pro- versus anti-tumor immunity. Cancer Metastasis Rev. 2010;29(2):309-16.
9. Murdoch C, Muthana M, Coffelt SB, Lewis CE. The role of myeloid cells in the promotion of tumour angiogenesis. Nat Rev Cancer. 2008;8(8):618-31.
10. Qian BZ, Pollard JW. Macrophage diversity enhances tumor progression and metastasis. Cell. 2010;141(1):39-51.
11. Salk JJ, Fox EJ, Loeb LA. Mutational heterogeneity in human cancers: origin and consequences. Annu Rev Pathol. 2010;5:51-75.
12. World-Health-Organization. Breast Cancer: Estimated Incidence, Mortality and Prevalence Worldwide in 2012: GLOBOCAN; 2012 [cited 2016 10.04]. Available from: Ferlay J, Soerjomataram I, Ervik M, Dikshit R, Eser S, Mathers C, Rebelo M, Parkin DM, Forman D, Bray, F.
13. KREFT-registeret. KREFTSTATISTIKK 2015 [cited 2016 10.04]. Available from: https://www.kreftregisteret.no/Registrene/Kreftstatistikk/.
14. Dumitrescu RG, Cotarla I. Understanding breast cancer risk -- where do we stand in 2005? J Cell Mol Med. 2005;9(1):208-21.
15. Marieb EN, Hoehn KN. Human Anatomy and Physiology. Ninth ed: Pearson; 2013.
16. Rochester-Medical-Center. Anatomy of the female breast 2016 [Available from: https://www.urmc.rochester.edu/Encyclopedia/Content.aspx?ContentTypeID=85&ContentID=P00132.
17. American-Cancer-Society. Types of breast cancers 2014 [07.04.2016]. Available from: http://www.cancer.org/cancer/breastcancer/detailedguide/breast-cancer-breast-cancer-types.
18. Chen S, Parmigiani G. Meta-analysis of BRCA1 and BRCA2 penetrance. J Clin Oncol. 2007;25(11):1329-33.
19. Breastcancer.org. HER2 Status 2016 [cited 2016 04.04]. Available from: http://www.breastcancer.org/symptoms/diagnosis/her2.

20. Mitri Z, Constantine T, O'Regan R. The HER2 Receptor in Breast Cancer: Pathophysiology, Clinical Use, and New Advances in Therapy. Chemother Res Pract. 2012;2012:743193.
21. Madarnas Y, Trudeau M, Franek JA, McCready D, Pritchard KI, Messersmith H. Adjuvant/neoadjuvant trastuzumab therapy in women with HER-2/neu-overexpressing breast cancer: a systematic review. Cancer Treat Rev. 2008;34(6):539-57.
22. Breastcancer.org. Understanding Hormone Receptors 2014 [cited 2016 04.04.]. Available from: http://www.breastcancer.org/symptoms/diagnosis/hormone_status/treatment_hrpos.
23. American-Cancer-Society. How is breast cancer classified? 2014 [cited 2016 05.04.]. Available from: http://www.cancer.org/cancer/breastcancer/detailedguide/breast-cancer-classifying.
24. Foulkes WD, Smith IE, Reis-Filho JS. Triple-negative breast cancer. N Engl J Med. 2010;363(20):1938-48.
25. Hudis CA, Gianni L. Triple-negative breast cancer: an unmet medical need. Oncologist. 2011;16 Suppl 1:1-11.
26. O'Shaughnessy J. Extending survival with chemotherapy in metastatic breast cancer. Oncologist. 2005;10 Suppl 3:20-9.
27. Redig AJ, McAllister SS. Breast cancer as a systemic disease: a view of metastasis. J Intern Med. 2013;274(2):113-26.
28. Weigelt B, Peterse JL, van 't Veer LJ. Breast cancer metastasis: markers and models. Nat Rev Cancer. 2005;5(8):591-602.
29. Koo JS, Jung W, Jeong J. Metastatic breast cancer shows different immunohistochemical phenotype according to metastatic site. Tumori. 2010;96(3):424-32.
30. Guise T. Examining the metastatic niche: targeting the microenvironment. Semin Oncol. 2010;37 Suppl 2:S2-14.
31. Kalluri R, Weinberg RA. The basics of epithelial-mesenchymal transition. J Clin Invest. 2009;119(6):1420-8.
32. Lamouille S, Xu J, Derynck R. Molecular mechanisms of epithelial-mesenchymal transition. Nat Rev Mol Cell Biol. 2014;15(3):178-96.
33. Hazan RB, Phillips GR, Qiao RF, Norton L, Aaronson SA. Exogenous expression of N-cadherin in breast cancer cells induces cell migration, invasion, and metastasis. J Cell Biol. 2000;148(4):779-90.
34. Onder TT, Gupta PB, Mani SA, Yang J, Lander ES, Weinberg RA. Loss of E-cadherin promotes metastasis via multiple downstream transcriptional pathways. Cancer Res. 2008;68(10):3645-54.
35. Kohya N, Kitajima Y, Jiao W, Miyazaki K. Effects of E-cadherin transfection on gene expression of a gallbladder carcinoma cell line: repression of MTS1/S100A4 gene expression. Int J Cancer. 2003;104(1):44-53.
36. Sceneay J, Smyth MJ, Moller A. The pre-metastatic niche: finding common ground. Cancer Metastasis Rev. 2013;32(3-4):449-64.
37. Sceneay J, Parker BS, Smyth MJ, Moller A. Hypoxia-driven immunosuppression contributes to the pre-metastatic niche. Oncoimmunology. 2013;2(1):e22355.
38. Feldmann HJ, Molls M, Vaupel P. Blood flow and oxygenation status of human tumors. Clinical investigations. Strahlenther Onkol. 1999;175(1):1-9.

39. Vaupel P, Kelleher DK, Hockel M. Oxygen status of malignant tumors: pathogenesis of hypoxia and significance for tumor therapy. Semin Oncol. 2001;28(2 Suppl 8):29-35.
40. Michieli P. Hypoxia, angiogenesis and cancer therapy: to breathe or not to breathe? Cell Cycle. 2009;8(20):3291-6.
41. Harris AL. Hypoxia--a key regulatory factor in tumour growth. Nat Rev Cancer. 2002;2(1):38-47.
42. Vaupel P, Mayer A, Hockel M. Tumor hypoxia and malignant progression. Methods Enzymol. 2004;381:335-54.
43. Hockel M, Vaupel P. Tumor hypoxia: definitions and current clinical, biologic, and molecular aspects. J Natl Cancer Inst. 2001;93(4):266-76.
44. Liao D, Johnson RS. Hypoxia: a key regulator of angiogenesis in cancer. Cancer Metastasis Rev. 2007;26(2):281-90.
45. Ryan HE, Poloni M, McNulty W, Elson D, Gassmann M, Arbeit JM, et al. Hypoxia-inducible factor-1alpha is a positive factor in solid tumor growth. Cancer Res. 2000;60(15):4010-5.
46. Semenza GL. Targeting HIF-1 for cancer therapy. Nat Rev Cancer. 2003;3(10):721-32.
47. Zhong H, De Marzo AM, Laughner E, Lim M, Hilton DA, Zagzag D, et al. Overexpression of hypoxia-inducible factor 1alpha in common human cancers and their metastases. Cancer Res. 1999;59(22):5830-5.
48. Berra E, Milanini J, Richard DE, Le Gall M, Vinals F, Gothie E, et al. Signaling angiogenesis via p42/p44 MAP kinase and hypoxia. Biochem Pharmacol. 2000;60(8):1171-8.
49. Dang CV, Semenza GL. Oncogenic alterations of metabolism. Trends Biochem Sci. 1999;24(2):68-72.
50. Suzuki H, Tomida A, Tsuruo T. Dephosphorylated hypoxia-inducible factor 1alpha as a mediator of p53-dependent apoptosis during hypoxia. Oncogene. 2001;20(41):5779-88.
51. Dong Z, Venkatachalam MA, Wang J, Patel Y, Saikumar P, Semenza GL, et al. Up-regulation of apoptosis inhibitory protein IAP-2 by hypoxia. Hif-1-independent mechanisms. J Biol Chem. 2001;276(22):18702-9.
52. Chaudary N, Hill RP. Hypoxia and metastasis. Clin Cancer Res. 2007;13(7):1947-9.
53. Chang J, Erler J. Hypoxia-mediated metastasis. Adv Exp Med Biol. 2014;772:55-81.
54. Higgins DF, Kimura K, Bernhardt WM, Shrimanker N, Akai Y, Hohenstein B, et al. Hypoxia promotes fibrogenesis in vivo via HIF-1 stimulation of epithelial-to-mesenchymal transition. J Clin Invest. 2007;117(12):3810-20.
55. Jiang J, Tang YL, Liang XH. EMT: a new vision of hypoxia promoting cancer progression. Cancer Biol Ther. 2011;11(8):714-23.
56. Chaffer CL, Thompson EW, Williams ED. Mesenchymal to epithelial transition in development and disease. Cells Tissues Organs. 2007;185(1-3):7-19.
57. Moen I, Oyan AM, Kalland KH, Tronstad KJ, Akslen LA, Chekenya M, et al. Hyperoxic treatment induces mesenchymal-to-epithelial transition in a rat adenocarcinoma model. PLoS One. 2009;4(7):e6381.

58. Hockel M, Schlenger K, Aral B, Mitze M, Schaffer U, Vaupel P. Association between tumor hypoxia and malignant progression in advanced cancer of the uterine cervix. Cancer Res. 1996;56(19):4509-15.
59. Fyles A, Milosevic M, Hedley D, Pintilie M, Levin W, Manchul L, et al. Tumor hypoxia has independent predictor impact only in patients with node-negative cervix cancer. J Clin Oncol. 2002;20(3):680-7.
60. Brown JM. Tumor hypoxia in cancer therapy. Methods Enzymol. 2007;435:297-321.
61. Gray LH, Conger AD, Ebert M, Hornsey S, Scott OC. The concentration of oxygen dissolved in tissues at the time of irradiation as a factor in radiotherapy. Br J Radiol. 1953;26(312):638-48.
62. Tibbles PM, Edelsberg JS. Hyperbaric-oxygen therapy. N Engl J Med. 1996;334(25):1642-8.
63. Kulikovsky M, Gil T, Mettanes I, Karmeli R, Har-Shai Y. Hyperbaric oxygen therapy for non-healing wounds. Isr Med Assoc J. 2009;11(8):480-5.
64. Sahni T, Hukku S, Jain M, Prasad A, Prasad R, Singh K. Recent Advances in Hyperbaric Oxygen Therapy Medicine Update. 2004;14:632-9.

65. Gill AL, Bell CN. Hyperbaric oxygen: its uses, mechanisms of action and outcomes. QJM. 2004;97(7):385-95.
66. Boykin JV. How hyperbaric oxygen therapy helps heal chronic wounds. Nursing. 2002;32(6):24.
67. Bennett PB, Elliot H, Elliot DH. The Physiology and Medicine of Diving. London: W.B Saunders Company Ltd; 2003.
68. Undersea&Hyperbaric-Medical-Society. Indicationf for Hyperbaric Therapy 2016 [cited 2016 02.05]. Available from: https://www.uhms.org/resources/hbo-indications.html.
69. Wattel F, Mathieu D, Neviere R, Bocquillon N. Acute peripheral ischaemia and compartment syndromes: a role for hyperbaric oxygenation. Anaesthesia. 1998;53 Suppl 2:63-5.
70. Feldmeier J, Carl U, Hartmann K, Sminia P. Hyperbaric oxygen: does it promote growth or recurrence of malignancy? Undersea Hyperb Med. 2003;30(1):1-18.
71. Daruwalla J, Christophi C. Hyperbaric oxygen therapy for malignancy: a review. World J Surg. 2006;30(12):2112-31.
72. Moen I, Stuhr LE. Hyperbaric oxygen therapy and cancer--a review. Target Oncol. 2012;7(4):233-42.
73. Stuhr LE, Raa A, Oyan AM, Kalland KH, Sakariassen PO, Petersen K, et al. Hyperoxia retards growth and induces apoptosis, changes in vascular density and gene expression in transplanted gliomas in nude rats. J Neurooncol. 2007;85(2):191-202.
74. DuPre SA, Redelman D, Hunter KW, Jr. The mouse mammary carcinoma 4T1: characterization of the cellular landscape of primary tumours and metastatic tumour foci. Int J Exp Pathol. 2007;88(5):351-60.
75. Cailleau R, Young R, Olive M, Reeves WJ, Jr. Breast tumor cell lines from pleural effusions. J Natl Cancer Inst. 1974;53(3):661-74.
76. Tao K, Fang M, Alroy J, Sahagian GG. Imagable 4T1 model for the study of late stage breast cancer. BMC Cancer. 2008;8:228.
77. Pulaski BA, Ostrand-Rosenberg S. Mouse 4T1 breast tumor model. Curr Protoc Immunol. 2001;Chapter 20:Unit 20 2.

78. Iorns E, Drews-Elger K, Ward TM, Dean S, Clarke J, Berry D, et al. A new mouse model for the study of human breast cancer metastasis. PLoS One. 2012;7(10):e47995.
79. Fantozzi A, Christofori G. Mouse models of breast cancer metastasis. Breast Cancer Res. 2006;8(4):212.
80. Richmond A, Su Y. MOUSE XENOGRAFT MODELS VS GEM MODELS FOR HUMAN CANCER THERAPEUTICS. Dis Model Mech. 2008;1(2-3):78-82.
81. Price JE. Metastasis from human breast cancer cell lines. Breast Cancer Res Treat. 1996;39(1):93-102.
82. Yang S, Zhang JJ, Huang XY. Mouse models for tumor metastasis. Methods Mol Biol. 2012;928:221-8.
83. Price JE, Polyzos A, Zhang RD, Daniels LM. Tumorigenicity and metastasis of human breast carcinoma cell lines in nude mice. Cancer Res. 1990;50(3):717-21.
84. Francia G, Cruz-Munoz W, Man S, Xu P, Kerbel RS. Mouse models of advanced spontaneous metastasis for experimental therapeutics. Nat Rev Cancer. 2011;11(2):135-41.
85. Vernon AE, Bakewell SJ, Chodosh LA. Deciphering the molecular basis of breast cancer metastasis with mouse models. Rev Endocr Metab Disord. 2007;8(3):199-213.
86. Raa A, Stansberg C, Steen VM, Bjerkvig R, Reed RK, Stuhr LE. Hyperoxia retards growth and induces apoptosis and loss of glands and blood vessels in DMBA-induced rat mammary tumors. BMC Cancer. 2007;7:23.
87. Moen I, Jevne C, Wang J, Kalland KH, Chekenya M, Akslen LA, et al. Gene expression in tumor cells and stroma in dsRed 4T1 tumors in eGFP-expressing mice with and without enhanced oxygenation. BMC Cancer. 2012;12:21.
88. Al-Waili NS, Butler GJ, Beale J, Hamilton RW, Lee BY, Lucas P. Hyperbaric oxygen and malignancies: a potential role in radiotherapy, chemotherapy, tumor surgery and phototherapy. Med Sci Monit. 2005;11(9):RA279-89.
89. Close DM, Xu T, Sayler GS, Ripp S. In vivo bioluminescent imaging (BLI): noninvasive visualization and interrogation of biological processes in living animals. Sensors (Basel). 2011;11(1):180-206.
90. Dothager RS, Flentie K, Moss B, Pan MH, Kesarwala A, Piwnica-Worms D. Advances in bioluminescence imaging of live animal models. Curr Opin Biotechnol. 2009;20(1):45-53.
91. Ando Y, Niwa K, Yamada N, Enumoto T, Irie T, Kubota H, et al. Firefly bioluminescence quantum yield and colour change by pH-sensitive green emission. Nature Photonics. 2008;2:44-7.
92. Troy T, Jekic-McMullen D, Sambucetti L, Rice B. Quantitative comparison of the sensitivity of detection of fluorescent and bioluminescent reporters in animal models. Mol Imaging. 2004;3(1):9-23.
93. Keyaerts M, Verschueren J, Bos TJ, Tchouate-Gainkam LO, Peleman C, Breckpot K, et al. Dynamic bioluminescence imaging for quantitative tumour burden assessment using IV or IP administration of D: -luciferin: effect on intensity, time kinetics and repeatability of photon emission. Eur J Nucl Med Mol Imaging. 2008;35(5):999-1007.
94. Inoue Y, Kiryu S, Izawa K, Watanabe M, Tojo A, Ohtomo K. Comparison of subcutaneous and intraperitoneal injection of D-luciferin for in vivo bioluminescence imaging. Eur J Nucl Med Mol Imaging. 2009;36(5):771-9.

95. Stuhr LE, Iversen VV, Straume O, Maehle BO, Reed RK. Hyperbaric oxygen alone or combined with 5-FU attenuates growth of DMBA-induced rat mammary tumors. Cancer Lett. 2004;210(1):35-40.
96. American-Type-Culture-Collection. Passage number effects in cell lines: Tech Bulletin; 2010 [cited 2016 22.06]. Available from: http://www.atcc.org/~/media/PDFs/Technical Bulletins/tb07.ashx.
97. Lin HK, Hu YC, Yang L, Altuwaijri S, Chen YT, Kang HY, et al. Suppression versus induction of androgen receptor functions by the phosphatidylinositol 3-kinase/Akt pathway in prostate cancer LNCaP cells with different passage numbers. J Biol Chem. 2003;278(51):50902-7.
98. Minn AJ, Gupta GP, Siegel PM, Bos PD, Shu W, Giri DD, et al. Genes that mediate breast cancer metastasis to lung. Nature. 2005;436(7050):518-24.
99. Minn AJ, Gupta GP, Padua D, Bos P, Nguyen DX, Nuyten D, et al. Lung metastasis genes couple breast tumor size and metastatic spread. Proc Natl Acad Sci U S A. 2007;104(16):6740-5.
100. Moen I, Jevne C, Wang J, Kalland K-H, Chekenya M, Akslen LA, et al. Tumor-stroma interactions in 4T1 mammary tumors with and without enhanced oxygenation. 2011.
101. Haroon AT, Patel M, Al-Mehdi AB. Lung metastatic load limitation with hyperbaric oxygen. Undersea Hyperb Med. 2007;34(2):83-90.
102. Daruwalla J, Christophi C. The effect of hyperbaric oxygen therapy on tumour growth in a mouse model of colorectal cancer liver metastases. Eur J Cancer. 2006;42(18):3304-11.
103. Daruwalla J, Greish K, Nikfarjam M, Millar I, Malcontenti-Wilson C, Iyer AK, et al. Evaluation of the effect of SMA-pirarubicin micelles on colorectal cancer liver metastases and of hyperbaric oxygen in CBA mice. J Drug Target. 2007;15(7-8):487-95.
104. Cavallaro U, Christofori G. Multitasking in tumor progression: signaling functions of cell adhesion molecules. Ann N Y Acad Sci. 2004;1014:58-66.
105. Lee JM, Dedhar S, Kalluri R, Thompson EW. The epithelial-mesenchymal transition: new insights in signaling, development, and disease. J Cell Biol. 2006;172(7):973-81.
106. Wendt MK, Taylor MA, Schiemann BJ, Schiemann WP. Down-regulation of epithelial cadherin is required to initiate metastatic outgrowth of breast cancer. Mol Biol Cell. 2011;22(14):2423-35.
107. Hazan RB, Kang L, Whooley BP, Borgen PI. N-cadherin promotes adhesion between invasive breast cancer cells and the stroma. Cell Adhes Commun. 1997;4(6):399-411.
108. Li K, He W, Lin N, Wang X, Fan QX. Downregulation of N-cadherin expression inhibits invasiveness, arrests cell cycle and induces cell apoptosis in esophageal squamous cell carcinoma. Cancer Invest. 2010;28(5):479-86.
109. Hulit J, Suyama K, Chung S, Keren R, Agiostratidou G, Shan W, et al. N-cadherin signaling potentiates mammary tumor metastasis via enhanced extracellular signal-regulated kinase activation. Cancer Res. 2007;67(7):3106-16.
110. Nieman MT, Prudoff RS, Johnson KR, Wheelock MJ. N-cadherin promotes motility in human breast cancer cells regardless of their E-cadherin expression. J Cell Biol. 1999;147(3):631-44.

111. Padua D, Massague J. Roles of TGFbeta in metastasis. Cell Res. 2009;19(1):89-102.
112. Dong A, Fang Y, Zhang L, Xie J, Wu X, Zhang L, et al. Caffeic acid 3,4-dihydroxy-phenethyl ester induces cancer cell senescence by suppressing twist expression. J Pharmacol Exp Ther. 2011;339(1):238-47.
113. Bhat-Nakshatri P, Appaiah H, Ballas C, Pick-Franke P, Goulet R, Jr., Badve S, et al. SLUG/SNAI2 and tumor necrosis factor generate breast cells with CD44+/CD24- phenotype. BMC Cancer. 2010;10:411.
114. Gjerdrum C, Tiron C, Hoiby T, Stefansson I, Haugen H, Sandal T, et al. Axl is an essential epithelial-to-mesenchymal transition-induced regulator of breast cancer metastasis and patient survival. Proc Natl Acad Sci U S A. 2010;107(3):1124-9.

# Appendix

## Appendix A. Buffer recipes for Western Blot protocol

Lysis buffer:

- 50 mM Tris-HCl (pH 7.4)
- 150 mM NaCl
- 1% Trition X one
- 1 EDTA-free cOmplete Mini tablet
- 1 PhosStop phophatase inhibitor

TBS (1x):

- 100 ml 10x TBS
- 1000 ml $ddH_2O$

TBS-T (1x):

- 100 ml 10x TBS
- 1000 ml $ddH_2O$
- 1 ml Tween®20

I-block buffer:

- 100 ml 10x TBS
- 1000 ml $ddH_2O$
- 2 g I-Block
- Warm until 70°C and cool down to 20°C
- 1 ml Tween®20
- 1 ml 20% NaN3 (0,2 g in 1 ml)
- 2,18g $MgCl_2*6H_2O$

Tris-HCL (Trizma® hydrochloride): Sigma Aldrich, Steinheim, Germany

NaCl (Sodium chloride): Mona Grønningen, University of Bergen

1% Trition X: X000, Sigma-Aldrich, Steinheim, Germany

EDTA-free cOmplete Mini tablet: Roche Diagnostics, Manheim, Germany

PhosStop phosphatase inhibitor: Roche Diagnostics, Manheim, Germany

TBS (10x): G-Biosciences, St.Louis, USA

I-Block: Tropix®, Applied Biosystems, Thermo Scientific, Bedford, USA

Tween®20: Sigma-Aldrich, Steinheim, Germany

$NaN_3$ (sodium azide): Sigma Aldrich, Steinheim, Germany

$MgCl_2*6H_2O$ (magnesium chloride hexahydrate): Sigma Aldrich, Steinheim, Germany